Taylor & Francis
Taylor & Francis Group

Virtual reconstruction of the skull of *Bernissartia fagesii* and current understanding of the neosuchian–eusuchian transition

Jeremy E. Martin, Thierry Smith, Céline Salaviale, Jerôme Adrien & Massimo Delfino

View supplementary material ☑

Published online: 17 Mar 2020.

Submit your article to this journal ☑

Article views: 148

View related articles ☑

View Crossmark data ☑

Taylor & Francis
Taylor & Francis Group

Check for updates

Virtual reconstruction of the skull of *Bernissartia fagesii* and current understanding of the neosuchian–eusuchian transition

Jeremy E. Martin[a]* iD, Thierry Smith[b] iD, Céline Salaviale[a], Jerôme Adrien[c] and Massimo Delfino[d,e] iD

[a]*Université de Lyon, ENS de Lyon, Université Claude Bernard Lyon 1, CNRS, UMR 5276 Laboratoire de Géologie de Lyon: Terre, Planètes, Environnement, F-69342 46 Allée d'Italie, Lyon, France;* [b]*Royal Belgian Institute of Natural Sciences, Directorate Earth and History of Life, Rue Vautier 29, B-1000 Brussels, Belgium;* [c]*Université de Lyon, INSA-Lyon, UMR CNRS 5510 MATEIS, 7 Avenue Jean Capelle, 69621, Villeurbanne Cedex, France;* [d]*Dipartimento di Scienze della Terra, Università di Torino, Via Valperga Caluso 35, 10125 Torino, Italy;* [e]*Institut Català de Paleontologia Miquel Crusafont, Universitat Autònoma de Barcelona, Edifici ICTAICP, Carrer de les Columnes s/n, Campus de la UAB, 08193 Cerdanyola del Vallès, Barcelona, Spain*

Since the description of *Isisfordia duncani*, a number of new extinct species and revisions of previously described species have prompted a variety of contradicting phylogenetic hypotheses on the topology of Neosuchia. As a consequence, a consensus on the rooting of Eusuchia in relation to other neosuchian clades has not been reached and the origin of the group remains unsettled. Exemplifying this, *Bernissartia fagesii*, from the Early Cretaceous of Belgium, has long been considered a key taxon for understanding the origin of Eusuchia, but more recent hypotheses found support for a more basal position, as an ally to goniopholidids, paralligatorids or atoposaurids. Because many details of the anatomy of the type specimen are hidden by glue and the sediment adhering to the fossils, a number of characters are pending confirmation. Based on computed tomography data, we extract bones of the cranium and mandibles, describe new characters and re-evaluate anatomical details in the lectotype specimen. Our phylogenetic analysis confirms that *B. fagesii* is a derived neosuchian, unrelated to atoposaurids, goniopholidids and paralligatorids. We recover *B. fagesii* and *Koumpiodontosuchus aprosdokiti* in a basal position within Eusuchia, together with Susisuchidae, a group of gondwanan neosuchians containing *Susisuchus* and *Isisfordia*, which here form a polytomy with Hylaeochampsidae. The presence/absence of pterygoid-bound internal choanae cannot be used to fully resolve relationships at the neosuchian–eusuchian transition because of the variability of this character even at the familial level, as recently reported within susisuchids and bernissartiids. There is no doubt that true eusuchians were present in Laurasia as early as the Early Cretaceous, the hylaeochampsid *Hylaeochampsa vectiana* being the oldest (Barremian) undoubted representative. But whether the Eusuchia were also present in southern landmasses depends on solving the phylogenetic position of susisuchids and other less known gondwanan forms within or outside Eusuchia.

Keywords: Eusuchia; Neosuchia; Cretaceous; Europe; phylogeny; ecology

Introduction

Semi-aquatic crocodylomorphs have been ubiquitous in freshwater ecosystems since at least the Cretaceous. Hypotheses on the origin of modern eusuchian crocodylomorphs rely on a stable phylogenetic framework at the neosuchian–eusuchian transition. A consensus on the content forming the base of Eusuchia is in constant flux and the interrelationships of several neosuchian groups remain unsettled. Phylogenetic hypotheses about the origin and evolution of modern members have been intensely debated since the description of the Cretaceous *Isisfordia duncani* from Australia, originally interpreted as the oldest eusuchian representative (Salisbury *et al.* 2006). Although a number of taxa from Gondwana were at that time known from poorly preserved specimens (Stromer

1933; Gasparini & Buffetaut 1980; Michard *et al.* 1990), the discovery of *Isisfordia duncani* shifted the general paradigm about the origin of eusuchians from northern to southern landmasses. Recently, *I. duncani* has been reinterpreted as a derived neosuchian (Turner & Pritchard 2015) opening the way for a reassessment of other neosuchian lineages (Turner 2015). Yet, a consensus on neosuchian relationships remains fragile with several lineages, including susisuchids, goniopholidids, atoposaurids, paralligatorids, pholidosaurids and dyrosaurids, characterized by labile phylogenetic positions (e.g. Leite & Fortier 2018). *Bernissartia fagesii* from the Lower Cretaceous of Belgium has often been, and is still, used as an outgroup taxon in phylogenetic analyses (e.g. Brochu 1999; Martin et al. 2016a; Sookias 2019) but recent hypotheses do not confidently solve its phylogenetic position, but propose

---

*Corresponding author. Email: jeremy.martin@ens-lyon.fr

several alternatives (e.g. Turner 2015; Turner & Pritchard 2015). The uncertain phylogenetic position of *B. fagesii* partly arises from its possessing a mixture of plesiomorphic and derived traits, as recognized by previous authors (Buffetaut 1975; Norell & Clark 1990; Turner & Pritchard 2015), as well as from its state of preservation.

The type series of *B. fagesii* is represented by two specimens (IRSNB R46 and IRSNB R118) recovered in 1879 from the Barremian–Aptian coal mine at Bernissart (Dollo 1883) from the same horizon as two specimens of the goniopholidid *Anteophthalmosuchus hooleyi* (Martin *et al.* 2016b) and many skeletons of the ornithopod *Iguanodon bernissartensis* (Godefroit *et al.* 2012). It is noteworthy that, contrary to previous assignments, one of the Lavalette historical drawings of the Bernissart crocodylomorphs probably does not correspond to Dollo's goniopholidid (Bultynck 1989; Martin *et al.* 2016b, fig. 2A) but to *B. fagesii* (IRSNB R46) before it was mounted for display. *B. fagesii* has been reported from several Cretaceous localities in Europe including England (Buffetaut & Ford 1979), Spain (Buscalioni *et al.* 1984; Buscalioni & Sanz 1990) and France (Mazin & Pouech 2008). Dollo (1883) described *B. fagesii* as a close ally to Eusuchia. This view has been contradicted by Buffetaut
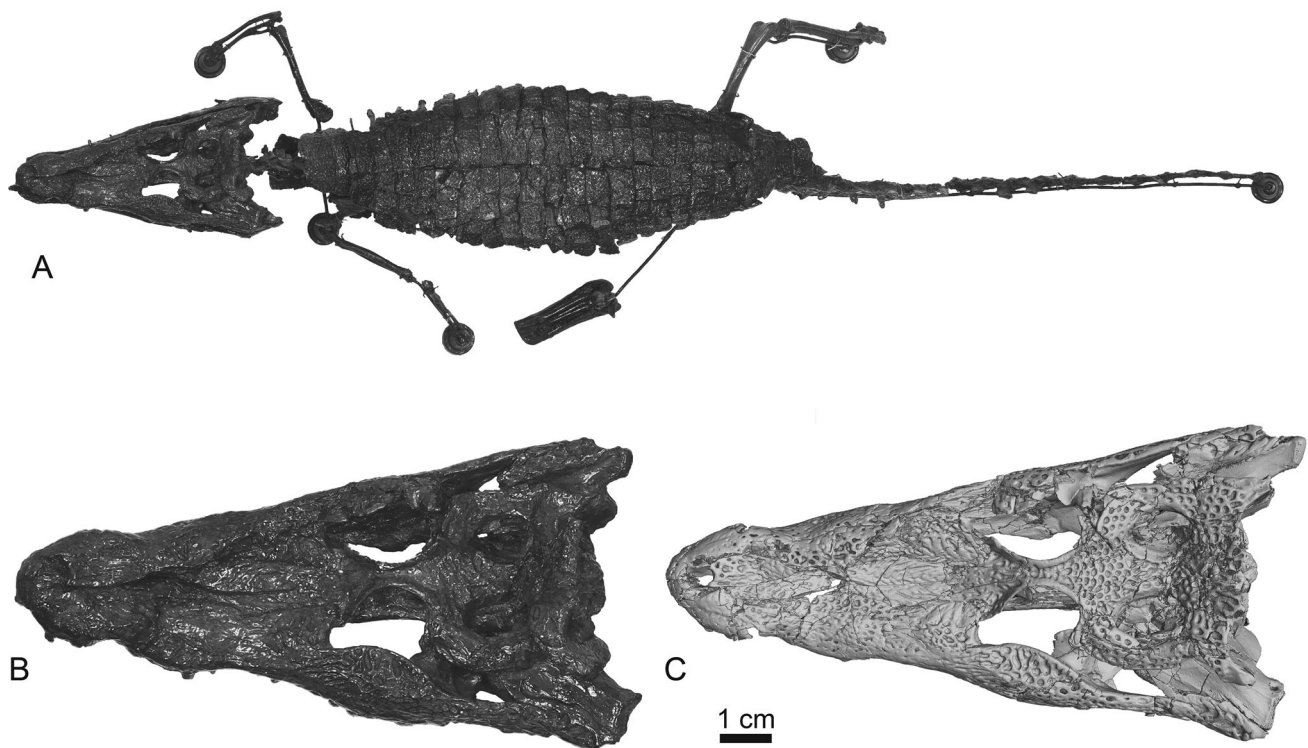
(1975); then it was partly defended (Norell & Clark 1990; Salisbury *et al.* 2006) viewing *B. fagesii* as an advanced neosuchian. More recent studies (Turner 2015; Turner & Pritchard 2015) presented two alternative hypotheses, with *B. fagesii* either as an outgroup to the crown group or as a member of Paralligatoridae.

The most comprehensive anatomical accounts of *B. fagesii* are those of Buffetaut (1975) and Norell & Clark (1990), both of which debate the position of the choanae. Allegedly, several characters are poorly preserved due to the crushed nature of the delicate historical specimen, which is covered by a layer of sediment and glue.

In order to solve this problem, we discuss new anatomical information derived from computed tomographic (CT) data of the lectotype specimen IRSNB R46 (Fig. 1), a nicely preserved cranium with mandibles. We explore its phylogenetic position and also take the opportunity to discuss the spatiotemporal distribution of Bernissartidae and their feeding ecology.

Institutional abbreviation

IRSNB: Institut Royal des Sciences Naturelles de Belgique, Brussels, Belgium.

Figure 1. The lectotype specimen of *Bernissartia fagesii* (IRSNB R46) from the Barremian–Aptian of Bernissart, Belgium. **A,** articulated skeleton in dorsal view. **B,** photograph of cranium in dorsal view compared with **C,** a virtual reconstruction using CT data. Note that virtually adjusting contrasts allows reconstruction of the specimen without glue or sediment. This also permits fine observations of anatomical details otherwise obscured by glows or poorly resolved contrast from the darkness of the specimen.

Material and methods

Computed tomographic scan parameters

The cranium and mandibles of IRSNB R46 (Dollo 1883) were scanned at the X-ray facility of the Laboratoire Mateis (INSA, Lyon) at a voxel size of 39 μm. The specimen was scanned with a vtomex laboratory X-ray computed tomograph (GE Phoenix | X-Ray GmbH) equipped with a 160 kV nano-focus tube, a tungsten transmitting target and a 1920 × 1536 pixel Varian detector. Scanning parameters were set to 140 kV tube voltage and 90 μA current with a voxel size of 39 μm. A single scan consists of 1200 2D radiographs and an averaging of five images at each step angle. The exposure time for one radiograph was 0.333 s. Three scans were performed in order to analyse the entire specimen. These parameters resulted in a measurement period of 2 h. The volume was reconstructed in phoenix datos|x (v. 2.1, GE Sensing & Inspection Technologies) using the conventional 2D filtered back projection algorithm. Volume rendering and processing of scans were completed with the Avizo software (Avizo Lite v. 9.0.1)

Phylogenetic analysis

Following our new observations, *Bernissartia fagesii* was entirely re-coded in a previously published matrix (Turner & Pritchard 2015) incorporating three new characters and totalling 345 characters and 66 taxa (see Supplementary Material). Because the present study focuses on derived neosuchians, Notosuchia and Thalattosuchia were not included in the analysis. We decided to exclude *Pachycheilosuchus trinquei* and *Gilchristosuchus palatinus* due to their fragmentary nature, the first being represented by a composite skeleton (Rogers 2003) and the second being represented by a partial skull table (Wu & Brinkman 1993). We coded the bernissartiid *Koumpiodontosuchus aprosdokiti* according to its recent description (Sweetman *et al.* 2014).

A phylogenetic analysis was performed using the software TNT v. 1.1. (Goloboff *et al.* 2008). A traditional search included replicates of 1000 random addition sequences (Wagner trees) followed by two rounds of TBR branch-swapping (10 trees retained by replication), the later one executed using the most parsimonious trees obtained in the first search and stored in the RAM.

Character definitions

Pholidosaurus and *Sarcosuchus* were recoded for ch. 49 as 49[0] according to previous observations of the cranioquadrate passage, which is open in these two taxa (Martin *et al.* 2016c). *Susisuchus anatoceps* was recoded as 49[2], as in *Isisfordia duncani*, following the observation provided in Salisbury *et al.* (2006). Following recent observations from Leite & Fortier (2018), codings for *Susisuchus anatoceps* were amended for the eusuchian type palate (ch. 43[1]) and procoelous condition in cervical vertebrae (ch. 92[1]).

One new state was added to character 207 (depression on posterolateral surface of maxilla: 2: expanding on jugal as maxillojugal depression) in order to match previous work on the maxillary depression among goniopholidids and pholidosaurids (Martin & Buffetaut 2012).

Three new characters were added. Character 343 (modified from character 414 in Martin et al. [2016c]): posterior margin of suborbital process of ectopterygoid in ventral view: straight or concave (0) or convex (1). Character 344 (modified from character 52 in Brochu [1999]): large, laterally displaced and adjoining maxillary and dentary alveoli holding double caniniform dentition: absent (0) or present (1). Character 345: posterior margin of the pterygoid wing: mediolaterally oriented (0) or posterolaterally oriented being straight or concave (1).

Systematic palaeontology

Crocodylomorpha Walker, 1970
Mesoeucrocodylia Whetstone & Whybrow, 1983
Neosuchia Benton & Clark, 1988
Bernissartiidae Dollo, 1883
Bernissartia Dollo, 1883
Bernissartia fagesii Dollo, 1883
(Figs 1–10)

Lectotype. IRSNB R46, an articulated skeleton, including a complete cranium with mandibles.

Locality and horizon. Coal mine of Bernissart, Belgium; Early Cretaceous, latest Barremian–earliest Aptian (after Yans *et al.* 2012).

Revised diagnosis. Updated from Buffetaut (1975) and Norell & Clark (1990). *Bernissartia fagesii* is a small neosuchian with a total body length less than 1 m and a mesorostrine skull with a rostrum to skull length ratio of 0.54. *B. fagesii* can be diagnosed by the following autapomorphies: presence of a peg on the lacrimal that interlocks with the maxilla; convex orbital margin of jugal. In addition, *B. fagesii* possesses the following combination of characters: nasals participating in the external nares; lacrimals slightly longer than the prefrontals; lacrimals contacting the nasals for a short distance; lacrimal with a smooth notch in its orbital margin; interorbital portion of frontal narrower than one orbital width; absence of periorbital ridge; quadratojugal

excludes quadrate from posterodorsal margin of lower temporal fenestra; foramen aereum opens on the dorso-medial edge of the quadrate; quadratojugal hides quadrate in lateral view; laterally opened cranioquadrate groove; supratemporal fenestrae smaller than orbits; long squamosals building more than two-thirds of the lateral margin of the skull table; squamosals with smooth posterior processes; frontoparietal suture within the level of the supratemporal fenestrae and participation of the frontals in the supratemporal fenestrae; small incisive foramen opening entirely into the premaxillae; narrow and elongated palatine branches that only slightly enter the maxillary palate; internal choanae bounded anteriorly by the palatines and posteriorly by the pterygoids; wide branches of the ectopterygoids with a straight suborbital margin; suborbital fenestrae longer than wide; lateral profile of upper and lower jaws sinusoidal; five premaxillary alveoli; 16 maxillary alveoli including large and closely spaced alveoli 4 and 5 for caniniform dentition; 20 dentary alveoli including large and confluent dentary alveoli $3+4$; tribodonty of last three maxillary and dentary teeth; last maxillary and dentary alveoli set in a groove; excavated pit at the premaxillary–maxillary suture for reception of the caniniform dentary teeth; short mandibular symphysis encompassing the first five dentary alveoli; splenial with modest participation into mandibular symphysis; presence of a bony shelf medial to the tribodont dentition in both the maxillae and splenials; retroarticular process in a ventral position relative to the jaw joint; thin ventral margin of the angular for the insertion of the M. pterygoideus posterior; absence of an external mandibular fenestra; amphicoelous cervical and thoracic vertebrae; biconvex first caudal vertebra; procoelous caudal vertebrae; dorsal osteoderms organized into a medial row that is wider than long and a lateral row that is square-like; double-keeled dorsal osteoderms on the medial row; single-keeled dorsal osteoderms on the lateral row; mediolaterally imbricated ventral osteoderms.

Description

General description and preservation

Bernissartia fagesii is a small taxon, the complete skeleton (IRSNB R46), as reconstructed, measuring a little more than 60 cm from the tip of the rostrum to the last preserved caudal vertebra. This total body length is within the range of other Cretaceous taxa known from complete skeletons that remain below or surpass 1 m long, such as *Isisfordia duncani*, *Susisuchus anatoceps*, *Pietraroiasuchus ormezanoi* and *Brillanceausuchus babouriensis* (Michard *et al.* 1990; Salisbury *et al.* 2003,

2006; Buscalioni *et al.* 2011). Several other Cretaceous taxa, known only from skulls, may not have surpassed this size range (*Acynodon*, *Theriosuchus*) whereas goniopholidids and perhaps paralligatorids were substantially larger (Martin *et al.* 2016b), but not attaining the observed size of *Allodaposuchus* (Martin *et al.* 2016a).

Bernissartia fagesii has been described previously as having a brevirostrine skull, but its rostrum to skull length ratio of 0.54 indicates a mesorostrine skull similar to that of *Allodaposuchus* (0.51 in the Velaux adult specimen) or *Diplocynodon* (*D. remensis* = 0.58) and slightly shorter than *Susisuchus anatoceps* (0.6), *Paralligator gradilifrons* (0.62), *Isisfordia duncani* (0.63) and *Pietraroiasuchus ormezanoi* (0.64). Goniopholidids have an even longer rostrum (0.67). On the other hand, brevirostrine taxa display a rostrum to skull length ratio <0.5 as in *Acynodon iberoccitanus* (0.4), *Koumpiodontosuchus aprosdokiti* (0.45) and *Iharkutosuchus makadii* (0.38). The rostrum proportions of *B. fagesii* depart from those of other typical 'shell crushers' in showing a slender rostrum. In *Bernissartia fagesii*, the rostrum is definitely not wide and short as in the hylaeochampsids *Acynodon*, *Allodaposuchus* or *Pietraroiasuchus*. In fact, its rostrum proportions are within the range of other mesorostrine forms such as *Isisfordia*, *Susisuchus*, *Koumpiodontosuchus* and *Paralligator*.

Digital removal of glue and sediment allows the cranium and mandibular ornamentation to be observed. The entire dorsal surface of the skull table, the quadratojugal, jugal, the bones forming the orbital margin and the median portion of the rostrum involving the nasal and medial-most parts of the maxilla are ornamented with marked ovoid pits. Such pits tend to be nearly circular and individualized on the squamosal, postorbital and lateral sides of the jugal, but are large and anastomosed on the quadratojugal and orbital margin of the jugal and are shallow and take the form of grooves on the rostrum. Most of the dorsal and lateral surfaces of the premaxillae and maxillae are nearly smooth, but deep, circular foramina open in a line just above the tooth row. In the mandible, the ornamentation contrasts between the dentary rami, where furrows and foramina dominate, and the posterior region, which is characterized by large anastomosed pits. Foramina densely cover the anterolateral and anteroventral portions of the dentary. Such foramina are sparsely distributed below the mandibular tooth row from the level of the sixth tooth back to the posterior tooth row area. Pits are wider and more circular on the lateral surface of the surangular than on the angular, where they make deep furrows near its posteroventral margin. The posterior mandibular edge made by the surangular and angular is devoid of ornamentation.

The cranium and mandible have been affected by crushing, as is often the case with bones embedded in

clay. The CT scans allow observations of numerous cracks in the internal structure of the specimen, to the point that most elements of the braincase cannot be reconstructed with the exception of the inner ear (see below). The cranium has clearly undergone dorsoventral compression, as evidenced by the rostrum sitting at the same level as the skull table and with the prefrontal pillars penetrating and distorting the palatines in their anterior portion. Some lateromedial skewing is also apparent in the cranium (Fig. 2I, J) and is obvious when comparing the left and right mandibular rami. In fact, the right mandible better preserves the original outline in lateral view whereas the left one has undergone deformation of the angular in two different parts (compare Fig. 2E and F).

Fenestrae and openings

The longer than wide external nares fully face dorsally and are delimited by the premaxillae and by the anterior nasal processes. Their posterior margin is imperfectly preserved because the paired nasals are partially displaced. The premaxillae contribute to the anterior and lateral contours of the external nares. These openings are slightly smaller than the supratemporal fenestrae. The small incisive foramen is almond-shaped and is contained within the palatal portion of the premaxillae, extending between the level of the second and fourth premaxillary alveoli. No antorbital fenestra or foramen could be identified. The orbits are delimited anteriorly by the lacrimals as a smooth notch, laterally by the jugals, medially by the prefrontals and frontal, and posteriorly by the postorbitals. The orbital outline, especially the lateral margin, has suffered from dorsoventral compression. Here, the crushed jugal gives a false impression of a concave lateral margin. The undeformed orbits may have been oval and anteroposteriorly elongated. The lacrimal contributing to the orbital margin shows a smooth surface, corresponding to a sulcus. Because of deformation, this sulcus gives a false impression of being prominent on the right lacrimal, but the left one shows the best-preserved condition with a limited extent. The suborbital fenestrae are elongated and extend for nearly the entire palatine length, anteriorly up to the level of the tenth maxillary alveolus. They are delimited anteriorly and laterally by the maxillae and posteriorly by the ectopterygoids. It is unclear whether the pterygoids contributed slightly to their posterior-most margins because the bones are loosely connected. The right suborbital fenestra best preserves its lateral margin, which is slightly convex at the level of the largest maxillary alveolus. The posterolateral margin of the suborbital fenestra joins the midline of the cranium along an oblique and straight ectopterygoid
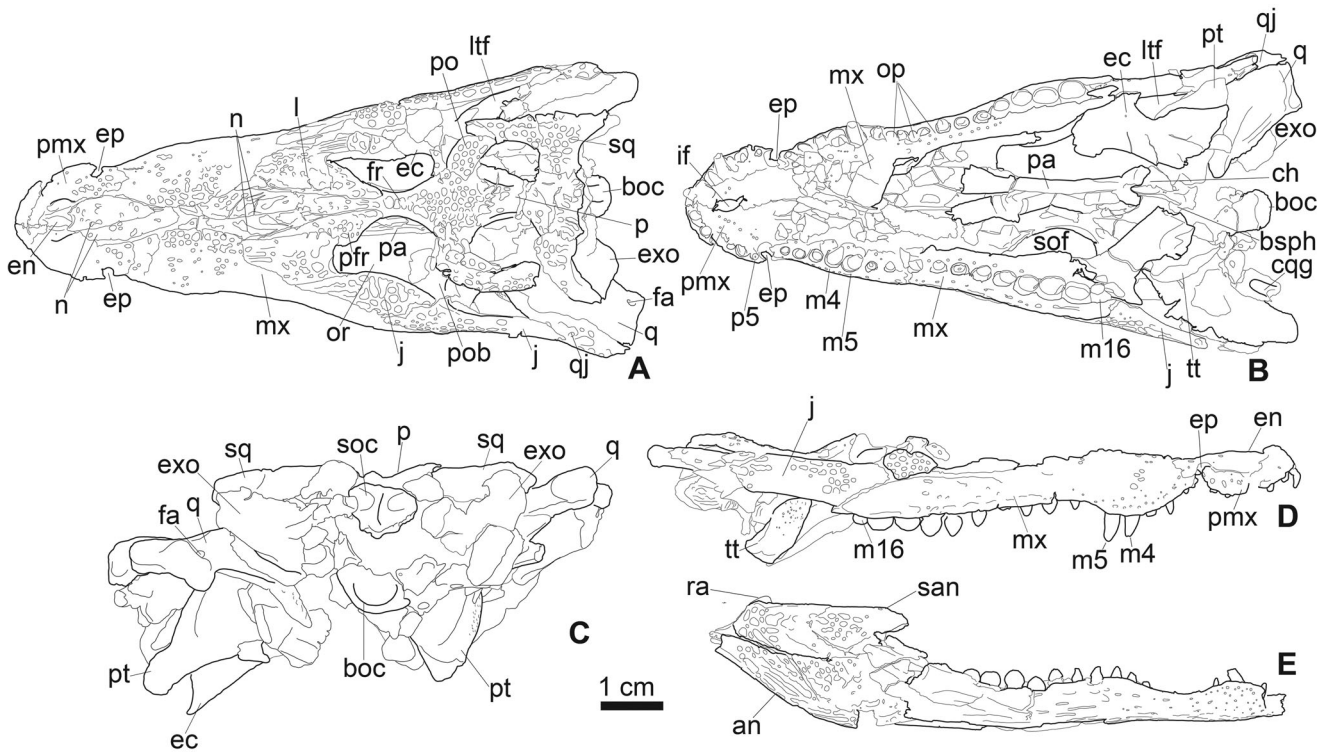
margin. The supratemporal fenestrae are ovoid, being slightly longer than wide. The anterior and anterolateral margins are composed of frontals and postorbitals, respectively. The squamosals form the lateral and posterior margins while the parietals make up the medial margins and contribute a little to the posteromedian margins. The internal supratemporal walls are vertical, except the anterior half of the parietal, which shows a smooth inclined surface. The supratemporal fenestrae are about half of the size of the orbits. The orbitotemporal foramina could not be identified due to the presence of numerous fractures. The lower temporal fenestrae face dorsolaterally and are delimited ventrally by the jugals, posteriorly by the quadratojugals and dorsally by the squamosals and postorbitals. They are longer than high and extend along the anterior half of the skull table. Little can be said about the outline of the foramen magnum due to bone fragmentation in the area. The exoccipitals form its lateral margins and it is uncertain whether the supraoccipital participates in the dorsal margin or whether the exoccipitals prevent such involvement. The ventral margin is formed by the basioccipital condyle. An external mandibular fenestra is absent, as evidenced from the sutural relationships of the surangulars, angulars and dentaries in the posterior margin of the lower jaw. The foramen intermandibularis oralis opens medially in the anterior portion of the splenial, at the level of the fifth dentary alveolus.

Rostrum

Both the left and right premaxillae are fractured but remain sutured to each other along the ventral margin and anterior to the external nares (Fig. 2). Each bone is longer than wide with a gently convex anterolateral contour. The dorsal surface is weakly ornamented; marked pits are visible just above the tooth row. The premaxillary dorsal process is partly eroded and delimits the external narial margin, which is bounded anteriorly and laterally by the premaxilla and posteriorly by the nasal. An anteroposteriorly directed sulcus extends on the dorsal surface of the premaxilla, just lateral to the external nares. The posterior premaxillary process is long and not as wide as the anterior portion of the premaxilla; contrary to the condition in other derived neosuchians, this premaxillary process attains the suture with the maxilla well posterior to the premaxillary–maxillary notch. The posterior premaxillary process consists of a thin lamina that overlies the maxilla. As observed externally, the premaxillary–maxillary suture is perpendicular to the rostrum.

As observed in ventral view, the premaxillae give a semicircular outline to the anterior margin of the rostrum. The incisive foramen consists of a small, longer

Figure 3. Line drawings of the cranium of *Bernissartia fagesii* (IRSNB R46) in **A,** dorsal, **B,** ventral, **C,** occipital and **D,** right lateral views. Associated right mandible in **E,** lateral view. Line drawing in C is not to scale and has been slightly augmented for clarity. **Abbreviations: an,** angular; **boc,** basioccipital; **ch,** choana; **cqg,** cranioquadrate groove; **ec,** ectopterygoid; **en,** external nares; **ep,** excavation pit; **exo,** exoccipital; **fa,** foramen aereum; **fr,** frontal; **if,** incisive foramen; **j,** jugal; **l,** lacrimal; **ltf,** lower temporal fenestra; **mx,** maxilla; **n,** nasal; **op,** occlusal pit; **or,** orbit; **p,** parietal; **pa,** palatine; **pfr,** prefrontal; **pmx,** premaxilla; **po,** postorbital; **pob,** postorbital bar; **pt,** pterygoid; **q,** quadrate; **qj,** quadratojugal; **ra,** retroarticular process; **san,** surangular; **soc,** supraoccipital; **sof,** suborbital fenestra; **sq,** squamosal; **tt,** torus transiliens of pterygoid; **p1–5,** premaxillary alveolar or tooth count; **m1–16,** maxillary alveolar or tooth count.

than wide, ovoid opening. It is completely enclosed by the premaxillae and opens away from the tooth row. The right and left premaxillae are in contact posterior to the incisive foramen through a long median palatal laminar suture, preventing any maxillary process from dividing the premaxillae. The lingual premaxillary alveolar walls are damaged but the teeth are still in position, allowing assessment of relative alveolar dimensions. There are five individualized alveoli per premaxilla; the first is separated from the second by a diastema; the third and fourth are the largest and

separated from each other by a deep occlusal pit. The fifth premaxillary alveolus is the smallest and its posterior margin is close to the premaxillary–maxillary notch. The premaxilla nearly encompasses this notch, although the anterior-most maxillary process participates in the posteroventral margin of the notch. This notch accommodates the large fourth caniniform dentary tooth, as evidenced by the mandible on the mounted specimen (Figs 2, 3). The premaxillary–maxillary notch marks the first festoon of the tooth row, giving a constricted outline to the upper jaw at this level. This circular notch is

Figure 2. 3D surface rendering of the cranium of *Bernissartia fagesii* (IRSNB R46) in **A,** dorsal, **B,** ventral, **C,** left lateral and **D,** right lateral views. Associated left mandible in **E,** lateral and **F,** medial views. Associated right mandible in **G,** medial and **H,** lateral views. **I, J,** both associated mandibles in occlusal and ventral views, respectively and cranium in **K,** anterior and **L,** occipital views. **Abbreviations: agf,** articular glenoid fossa; **an,** angular; **art,** articular; **boc,** basioccipital; **bsph,** basisphenoid; **co,** coronoid; **cqg,** cranioquadrate groove; **den,** dentary; **ec,** ectopterygoid; **en,** external nares; **ep,** excavation pit; **exo,** exoccipital; **fa,** foramen aereum; **fio,** foramen intermandibularis oralis; **fr,** frontal; **if,** incisive foramen; **j,** jugal; **l,** lacrimal; **ltf,** lower temporal fenestra; **mmf,** medial mandibular fenestra; **mx,** maxilla; **n,** nasal; **op,** occlusal pit; **or,** orbit; **p,** parietal; **pa,** palatine; **pfr,** prefrontal; **pmx,** premaxilla; **po,** postorbital; **pob,** postorbital bar; **pt,** pterygoid; **q,** quadrate; **qj,** quadratojugal; **ra,** retroarticular process; **san,** surangular; **soc,** supraoccipital; **sof,** suborbital fenestra; **sp,** splenial; **sq,** squamosal; **sym,** symphysis; **tt,** torus transiliens of pterygoid; **p1–5,** premaxillary alveolar or tooth count; **m1–16,** maxillary alveolar or tooth count; **d1–d20,** dentary alveolar or tooth count.
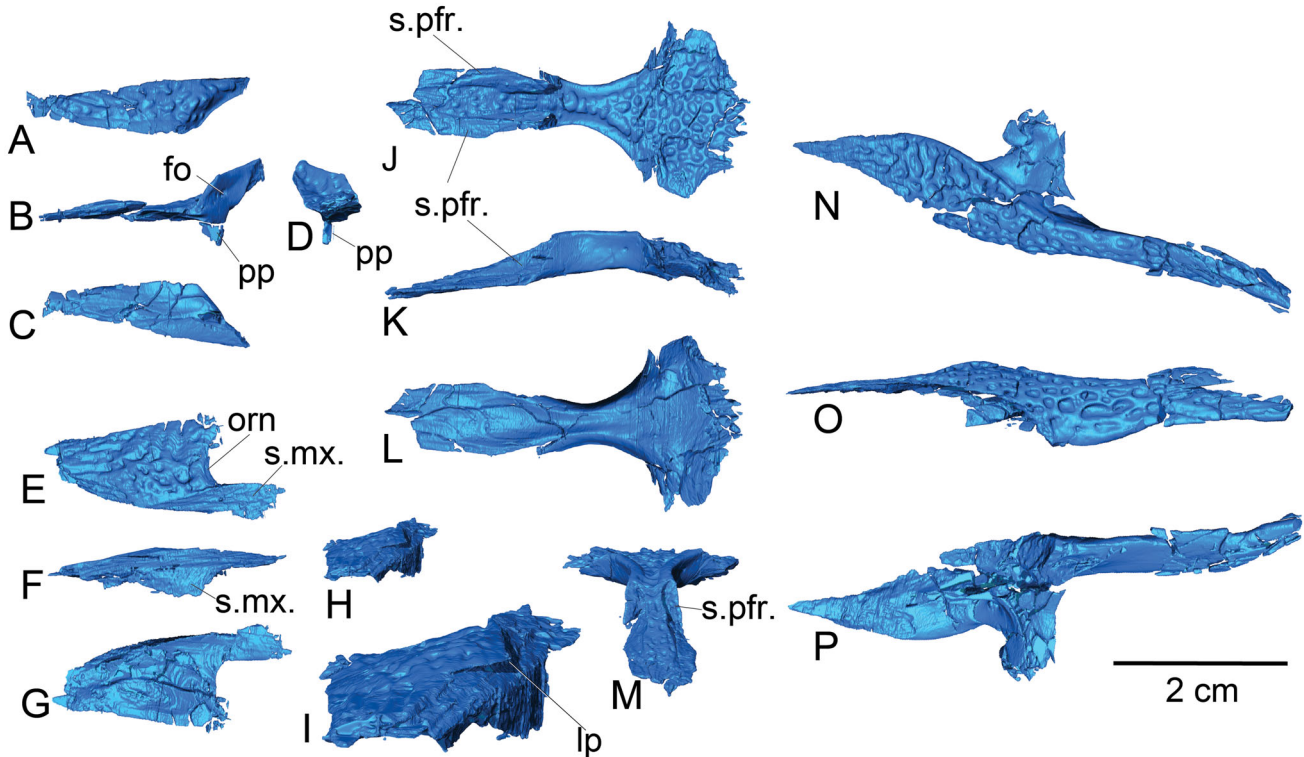
close to being excavated laterally, indicating that onto-genetically old specimens should present a complete excavation of the notch. Here, on both sides of the cranium, the premaxillae and maxillae possess bony projections that nearly meet along the lateral margin of the rostrum (Fig. 2). Therefore, when occluding in the premaxillary–maxillary notch, the enlarged dentary tooth crown becomes partly visible in lateral view. An oblique line of small foramina pierces the ventral surface of the premaxilla. Occlusal pits in the maxilla are obvious between the sixth and seventh, between the seventh and eighth, and between the eighth and ninth alveoli. The first two anterior pits are located in the interalveolar spaces and indicate an interdigitated occlusion (Figs 2, 3). The last of these occlusal pits is slightly offset lingually. Faint occlusal pits can also be detected between the ninth and thirteenth alveoli.

The maxillae contribute to most of the rostrum. As evidenced from both sides, there are 16 maxillary alveoli. In lateral view, the maxillae display a marked double wave, attaining a maximum convexity at the level of the double caniniform dentition as well as at the level of the posterior molariform teeth. The maxillae do not suture medially on the dorsal surface, being separated by the nasals along an extensive suture. Although the ventral surface is heavily fractured, the maxillae seem to suture to each other from the level of the premaxillary suture to the level of the eighth or ninth maxillary alveoli. In dorsal view, the maxillae have extensive sutural contacts with the lacrimals and jugal along their posteromedian margins. The maxillae extend posteriorly to underlie the entire lengths of the orbits, but do not participate in the orbital margins. Ventrally, the posteromedian maxillary suture of the palate appears separated by the anterior palatine processes for a short distance, but this area is poorly preserved. The posterior part of the maxilla possesses a distinct median shelf that projects within the suborbital fenestra, at the level of the large molariform (fourteenth) alveolus. From this point, the posteromedian maxillary margin sutures extensively with the anterior ectopterygoid process. The last maxillary alveolus is close but contacts neither the ectopterygoid, nor the jugal. The jugal articulates with the posterior-most margin of the maxilla. The paired nasals can be observed in dorsal view and extend for nearly the entire length of the rostrum. Their posterior extent, in front of the orbits, connects with the anterior frontal process as well as with a long prefrontal process along their posteromedial margins. Anterior to the prefrontal contact, the nasals contact the lacrimal anterior processes for a short distance. Most of the lateral margins of the nasals contact the maxillae. The nasals become narrow at the level of the large caniniform maxillary alveoli. Anterior to this point, they become wide and contact the premaxillae, where they participate in the posterior margin of the external nares, and a short spiny median process extends into the nares.

Periorbital area

The jugal extends along the lateral margin of the cranium between the maxilla and the quadratojugal. Its anterior process projects ahead of the orbits reaching the level of the thirteenth maxillary alveolus. Here, the jugal extensively overlaps the posterior margin of the maxilla and sutures along its anteromedial margin onto a dorsally facing suture of the lacrimal. The jugal orbital margin consists of a long and concave tongue that delimits an external ornamented surface from a smooth internal surface. Posterior to the orbit, the jugal contribution to the postorbital bar is medially inset from the external surface of the jugal. Its suture with the descending postorbital process is difficult to observe due to crushing and the presence of numerous cracks. The posterior jugal process is mediolaterally compressed and forms the ventral margin of the lower temporal fenestra. The jugal contacts the ascending process of the ectopterygoid below the level of the jugal contribution to the postorbital bar. No jugal foramen could be observed, but this may be due to poor preservation. The lacrimal is a flat bone, which is longer than wide, with an anterior region that is slightly narrower than its posterior region. It occupies the anterior orbital margin where it sends a posterolateral process into the orbit alongside the jugal. The lacrimal shares a long median suture with the prefrontal and, anteromedially, it contacts the nasal. Anteriorly and anterolaterally, the lacrimal sutures with the maxilla. Here, above the suture, the dorsal surface of the lacrimal possesses an anteriorly projecting peg that interlocks with the maxilla (Fig. 4H, I). The prefrontal is an elongate bone wedged between the lacrimal and the anterior frontal process. An elevated rim delimits the ornamented dorsal surface from the smooth vertical orbital margin, which is pierced by a single foramen. Most of the lateral margin is covered dorsally by the lacrimal. The anteromedial process of the prefrontal projects anteriorly, but not as far as the lacrimal. This process contacts the frontal extensively and the nasals medially. The prefrontal pillars descend ventrally from the orbital margin of the prefrontal to contact the palatines in their anterior region. The frontal bridges the skull table and the periorbital area. Its unpaired process contributes to the median orbital margin where it is rimmed by a thin crest. The frontal has a long anterior process that slopes anterior to the orbits. This process accommodates the prefrontal and projects underneath the nasals for a short distance. No periorbital ridge or

Figure 4. Bones from the antorbital area of *Bernissartia fagesii* (IRSNB R46). Left prefrontal in **A,** dorsal, **B,** lateral, **C,** ventral and **D,** anterior views. Left lacrimal in **E,** dorsal, **F,** lateral, **G,** ventral and **H, I,** anterior views. The view in I is an enlargement of the view in H and is not to scale. Frontal in **J,** dorsal, **K,** left lateral, **L,** ventral and **M,** anterior views. Left jugal in **N,** dorsal, **O,** lateral and **P,** ventral views. **Abbreviations: lp**, lacrimal peg; **fo**, foramen; **orn**, orbital notch; **pp**, prefrontal pillar; **s.mx.**, suture for maxilla; **s.pfr.**, suture for prefrontal.

crest is present. In its posterior portion, the frontal sutures laterally with the postorbital and posteriorly with the parietal along an interdigitated suture. The frontoparietal suture is located within the anterior half of the supratemporal fenestra. The frontal participates in the anteromedial corner of the supratemporal fenestra for a short distance. Here, the frontal sits over the capitate process of the laterosphenoid and the horizontal suture between them is visible in the anterior part of the supratemporal fenestra. In ventral view, the sulcus for the olfactory tract is well marked and the imprint corresponding to the olfactory bulbs is wider than the interorbital space.
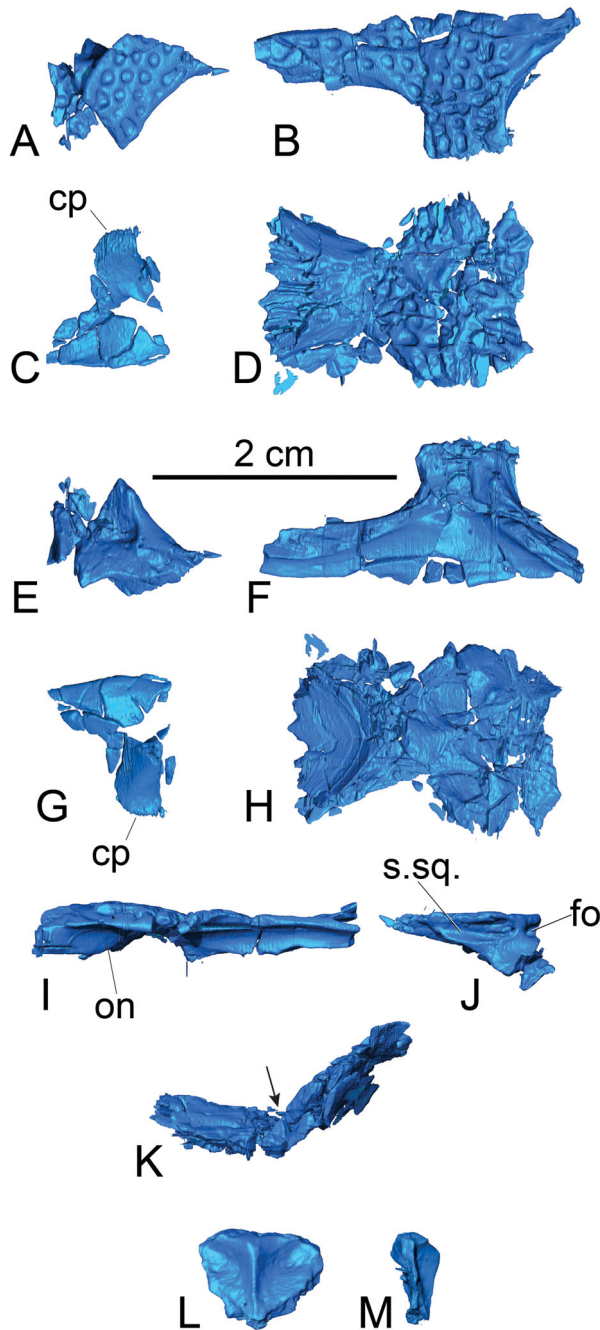
Skull table

The skull table is flat and devoid of a median crest on the frontoparietal midline. The frontoparietal suture is located between the supratemporal fenestrae and prevents contact between the parietal and postorbital. The parietal retains the same width between the supratemporal fenestrae and in its posterior part. This width is about the same as the supratemporal fenestra width. The

parietal delimits the posterior margin of the skull table and, as observed in dorsal view, prevents the supraoccipital from participating in the skull table. The postorbital is restricted to the anterolateral corner of the skull table. Just below the level of the skull table, a large foramen opens on the anterolateral margin of the postorbital bar (Fig. 5J). Almost reaching this foramen, the squamosal projects anteriorly as a strong acute process over the postorbital bar (Fig. 5J), which does not reach the orbital margin. The squamosal contributes to more than two-thirds of the length of the skull table. The squamosal projects posteriorly, with the dorsal surface of the squamosal lobe being flat and unsculpted.

Palate

The palatal region of the cranium underwent several breakages and its bones are slightly displaced but maintain their original positions. The left ectopterygoid is nearly complete and possesses a complex shape. The torsion of its main corpus has been attenuated by crushing. Its posterolateral flange is pointed and overlaps the pterygoid wing. Its posterior margin bears a notch. The main
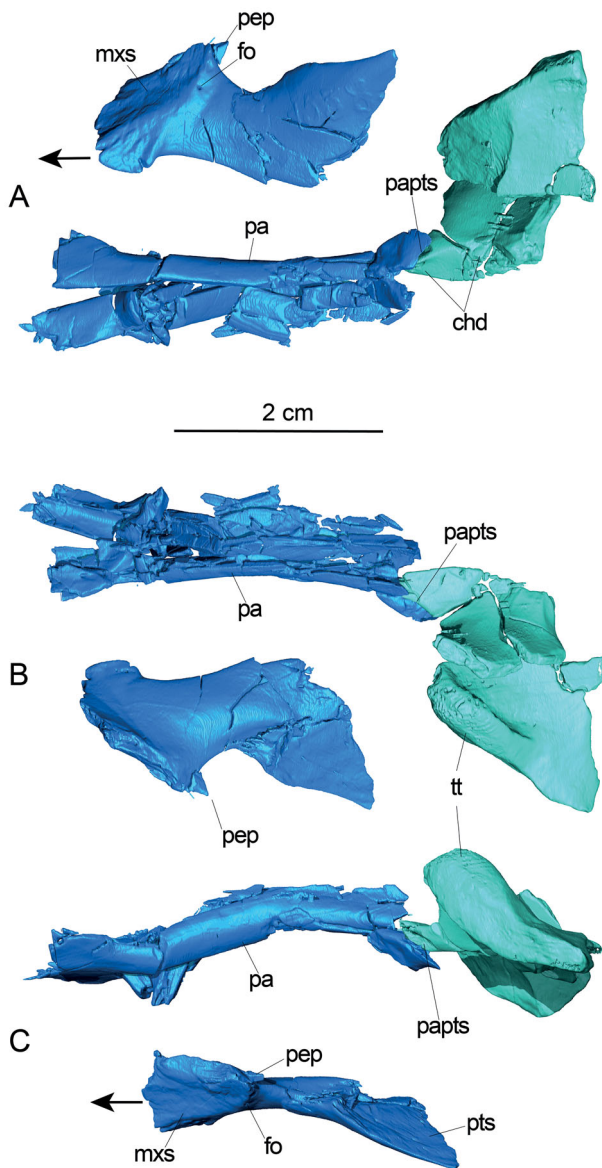
Figure 5. Elements of the skull table of *Bernissartia fagesii* (IRSNB R46) in **A–D,** dorsal, **E–H,** ventral, and **I–K,** right lateral views, with **A, E, J**, right postorbital, **B, F, I**, right squamosal, **C, G**, right laterosphenoid, and **D, H, K**, right parietal. The supraoccipital is presented in **L,** posterior and **M,** left lateral views. The arrow in **K** points to a fracture running through the deformed parietal. **Abbreviations: cp**, capitate process; **fo**, foramen; **on**, otic notch; **s.sq.**, suture for squamosal.

corpus is relatively wide and shows a foramen opening near the suture for the maxilla on its ventral side. In dorsal or ventral views, the ectopterygoid has sutural contacts

with the maxilla and pterygoid. Norell & Clark (1990) described the lateral part of the ectopterygoid as extending dorsally to contact the postorbital on the medial surface of the postorbital. The area is crushed but the left side shows instead that the ectopterygoid contacts the ventral surface of the jugal contribution to the postorbital bar, but not the postorbital itself, which is positioned slightly more dorsally (Fig. 6). A short ectopterygoid process extends along the medial surface of the jugal (Fig. 6). As noted previously by Buffetaut (1975) and Norell & Clark (1990), the left pterygoid appears to preserve the median suture contacting the right element, therefore confirming that the pterygoids meet posterior to the choanae. The morphology of the pterygoid is best exemplified by the left element, which is almost complete and appears triangular in outline. The lateral margin of the pterygoid flange is obliquely oriented relative to the anteroposterior axis of the cranium. It is extremely thick anteriorly, corresponding to the torus transiliens, which is expanded dorsally but not ventrally. Posterior to the torus transiliens, the lateral margin of the pterygoid flange projects posterolaterally as a thin lamina. Here, the posterior margin is thin and perpendicular to the anteroposterior axis of the cranium. As preserved, the posteromedian margin of the pterygoid flange is at a level more anterior than the posterolateral margin. The ventral margin of the pterygoid wing is flat and a shallow notch along the lateral margin indicates the lateral-most limit of the suture with the ectopterygoid.

The CT data allow clarification of some important features of the palate. The left pterygoid and palatine preserve a sutural contact and both contribute to the choanal opening (Figs 2, 3); the palatine contributes to the anterolateral margins of the choana, as a thin lamina contacting the pterygoid ventrally. The anterior margin of the choana reaches the level of the suborbital fenestrae, but does not penetrate far anteriorly within the interfenestral bars. The palatine bars are straight and parallel to each other for their entire lengths, occupying all of the median margins of the suborbital fenestrae (Figs 2, 6). The left palatine is the less fractured. As observed in ventral view, both palatines expand very slightly laterally into the maxillae, where their anteriormost extent reaches the level of the tenth maxillary alveolus. The internal part of the palatines is hollow, connecting the internal choanae with the external nares via a closed duct. Numerous breaks prevent us from assessing which bone contributes to the dorsal wall of this choanal duct. As observed by Norell & Clark (1990), the prefrontal pillars meet the palatines at about one-third of the distance from their anterior margins. This is visible due to crushing, where the right vertical pillar deforms the right palatine.

Figure 6. 3D surface rendering of left palatal elements of *Bernissartia fagesii* (IRSNB R46) in **A,** ventral, **B,** dorsal and **C,** left lateral views. Anterior is indicated by the arrow. **Abbreviations: chd,** choanal depression on pterygoid; **fo,** foramen; **mxs,** maxillary suture of the ectopterygoid; **pa,** palatine; **papts,** palatine–pterygoid suture; **pep,** posterior ectopterygoid process; **pts,** pterygoid suture of the ectopterygoid; **tt,** torus transiliens.
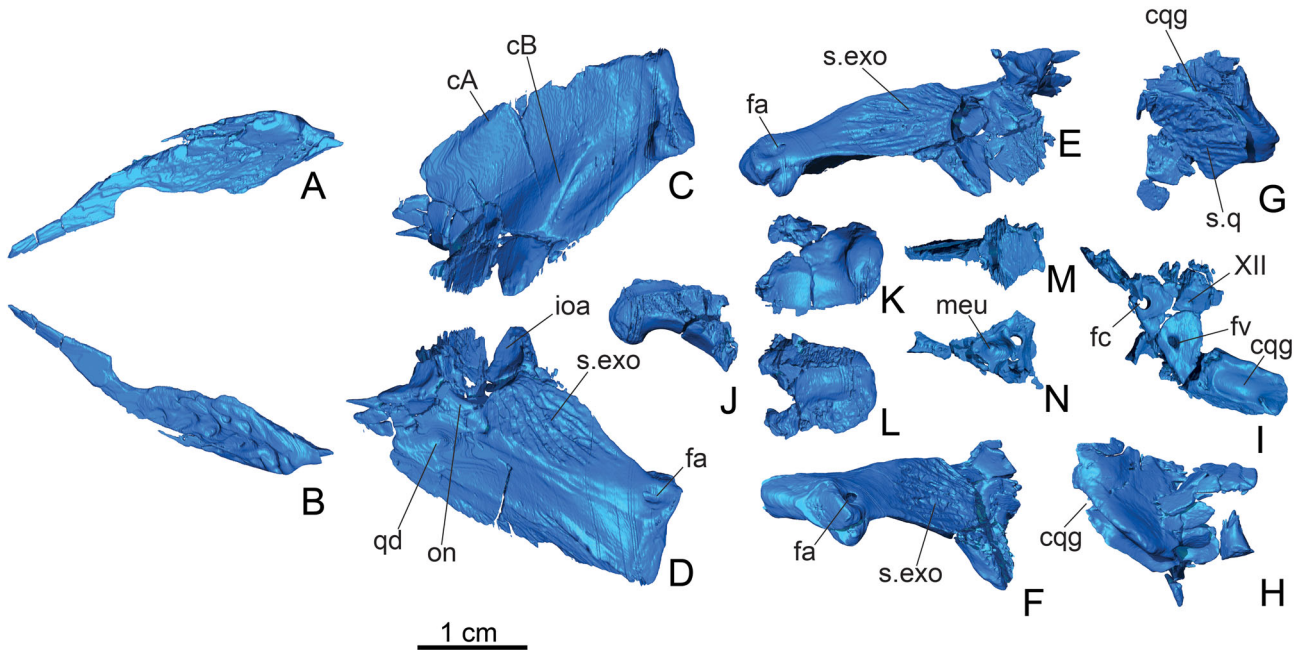
Braincase

The braincase is heavily fractured (Figs 7, 8), hampering inspection of the endocranial cavity and the orbitotemporal foramen. Nevertheless, the exit foramina for cranial nerve XII, the carotid artery and the vagal foramen are visible on the medial margin of the right exoccipital (Fig. 7). As evidenced from the left side, the
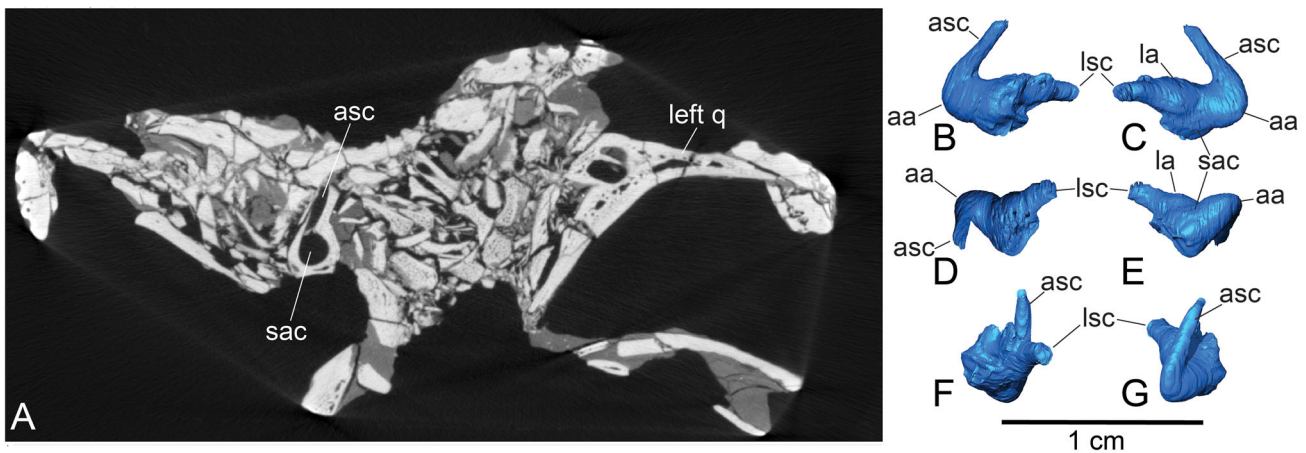
cranioquadrate passage is laterally open (Figs 2, 7G, H). This passage runs along the ventromedial margin of the exoccipital and only the exoccipital contributes to it. The posterior margin of the external otic aperture is delimited by a wide concave margin of the squamosal and exoccipital. The quadratojugal covers the lateral margin of the quadrate. The quadratojugal prevents the quadrate from participating in the posterodorsal corner of the lower temporal fenestra. The quadratojugal ascending process is best seen from the left side, but its dorsal-most tip is damaged and it is uncertain if it contacts the squamosal or the postorbital. The quadrate forms the ventral margin of the external otic aperture. Along its dorsal margin, the quadrate has one depression (Fig. 7D), as originally identified by Norell & Clark (1990). This depression is not perforated, although it is topologically similar to preotic sinuses, but other specimens will be required to investigate the relevance of this feature. The left quadrate condyle is complete and the foramen aereum opens on the dorsomedial corner of the quadrate (Fig. 7D–F). Muscle insertion scars are visible on the ventral surface of the quadrate branch (Fig. 7C). Here, a faint crest A (*sensu* Iordansky 1973) runs along the quadrate-quadratojugal suture. Crest B (*sensu* Iordansky 1973) is more strongly developed and extends obliquely in the middle of the posterior surface.

The supraoccipital is strongly developed above the foramen magnum and bears a strong vertical median keel (Fig. 5). The basioccipital contributes to the occipital condyle but the underlying basioccipital plate is destroyed. As preserved, the ventral-most process of the basisphenoid wedges between the pterygoid plates as a concave structure. Its dorsal portion is inflated and preserves the Eustachian canals. The median canal is the largest and the paired lateral foramina are located close to it near the posterior margin of the bone. The laterosphenoid preserves the capitate process, which is wider than long and contacts the frontal and, laterally, part of the postorbital as a rugose tubercle. On the lateral margin of the laterosphenoid, the cotylar crest is not developed. The trigeminal foramen is not preserved so it is not possible to assess whether a laterosphenoid bridge was present.

Due to heavy breakage in the endocranial cavity (Fig. 8A), the endosseous labyrinth could be partially reconstructed for the right side only. The cochlea could not be located but a partial vestibular system was reconstructed including parts of the lateral and anterior semicircular canals as well as the sacculus (Fig. 8B–G). The lateral semicircular canal is only preserved in its anterior region, where it connects to the anterior ampulla together with the anterior semicircular canal. Although the curvature of the lateral semicircular canal around the sacculus cannot be assessed precisely, its orientation
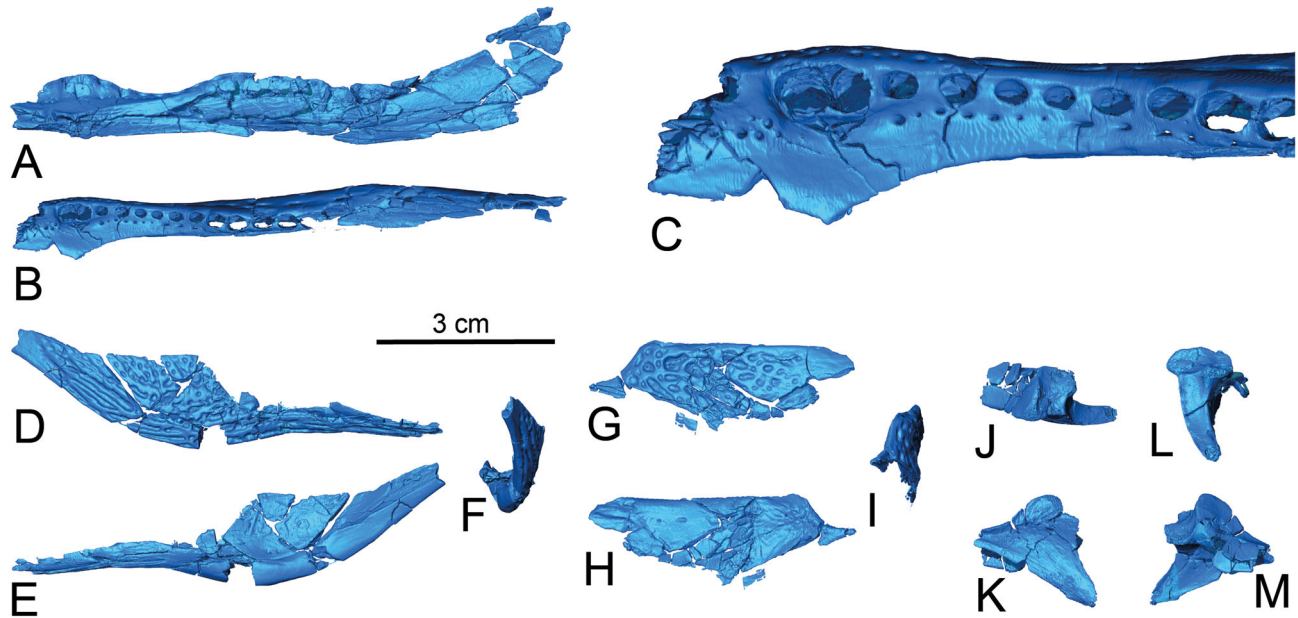
Figure 7. 3D surface rendering of braincase elements of *Bernissartia fagesii* (IRSNB R46) including the left quadratojugal in **A,** ventral and **B,** dorsal views. Left quadrate in **C,** ventral, **D,** dorsal, **E,** medial and **F,** posterior views. Left partially preserved exoccipital in **G,** anterior and **H,** posterior views. Right exoccipital in **I,** ventral view. Occipital condyle in **J,** right lateral, **K,** ventral and **L,** dorsal views. Basisphenoid in **M,** dorsal and **N,** ventral views. **Abbreviations: cA, cB,** crests A and B (*sensu* Iordansky 1973); **cqg,** cranioquadrate groove; **fa,** foramen aereum; **fc,** opening for carotid artery; **fv,** opening for vagal foramen; **ioa,** internal otic aperture; **meu,** median Eustachian opening; **on,** otic notch; **qd,** quadrate depression; **s.exo,** suture for exoccipital; **s.q,** suture for quadrate; **XII,** opening for cranial nerve XII.

Figure 8. A, transverse tomography through the cranium of *Bernissartia fagesii* (IRSNB R46) illustrating the state of preservation of the inner parts of the cranium at slice 2589/3105 with part of the right labyrinth identified. 3D surface rendering of the right vestibular system in **B,** medial, **C,** lateral, **D,** dorsal, **E,** ventral, **F,** posterior and **G,** anterior views. **Abbreviations: aa,** anterior ampulla; **asc,** anterior semicircular canal; **la,** lateral ampulla; **lsc,** lateral semicircular canal; **q,** quadrate; **sac,** sacculus.

suggests a significant curvature (Fig. 8D, G). Curved lateral semicircular canals have been described in modern eusuchians and may indicate sensitivity (Brusatte *et al.* 2016). In lateral view, the straight, uncurved anterior semicircular canal of *B. fagesii* resembles the general pyramidal appearance of semicircular canals in *Crocodylus johnstoni*, *Pelagosaurus* and other crocodylomorphs (Pierce *et al.* 2017). As observed in lateral view, the angle between the lateral and anterior semicircular canals is about 47°, whereas it is 50–60° in

Figure 9. Bones of the mandible of *Bernissartia fagesii* (IRSNB R46). Right dentary in **A,** medial and **B,** occlusal views and **C,** a close-up view of its anterior portion. Right angular in **D,** lateral; **E,** medial and **F,** posterior views. Right surangular in **G,** lateral, **H,** medial and **I,** posterior views. Right articular in **J,** dorsal, **K,** lateral, **L,** anterior and **M,** medial views.

modern eusuchians (see Brusatte *et al.* 2016, fig. 8). Although the anterior ampulla is dorsoventrally expanded in modern eusuchians, here it seems laterally bulging. The lateral ampulla is distinctly inflated, more so than in modern eusuchians, which again supports sensitivity to angular motion (Sipla & Spoor 2008).
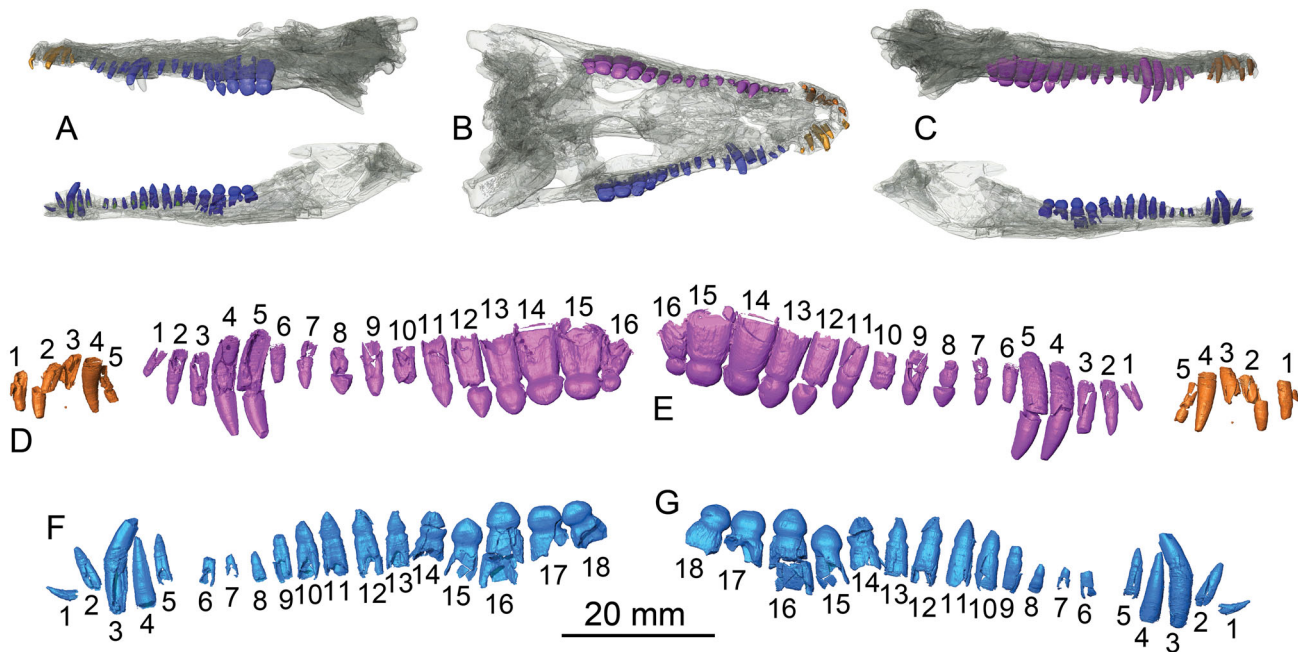
Mandible

In dorsal or ventral view, the mandible is 'V'-shaped, matching the triangular outline of the cranium (Fig. 2). The right dentary is damaged anteriorly but the left dentary is complete and includes a total of 18 alveoli (Figs 9, 10). The dentary is a long rod that makes up about three-quarters of the entire mandible length. In lateral view, the ventral surface of the dentary is flat and contrasts with the sinusoidal dorsal margin. As with the upper jaw, the dentary displays a typical double wave with maximum heights attained at the levels of dentary alveoli 3 + 4 and the twelfth dentary alveolus. The dentary symphyseal portion is spatulate and incorporates the first four alveoli. The splenial participates modestly in the mandibular symphysis. In dorsal or ventral view, the dentary narrows from the level of the fifth to the tenth alveoli. From the fourteenth alveolus posteriorly, the splenial contributes to the lingual wall of the dentary alveoli. Along the lateral side of the dentary, the bone is vertical but near its posterior end, it is slightly bulged at the level of the last alveolus. In lateral view, the dentary

has a large contact with the angular and, dorsally, contacts the surangular along a less extensive suture. The splenial prevents any contribution of the dentary to the lingual cavity. The first dentary alveolus is damaged but the left tooth is preserved in position and is procumbent. The second alveolus is set apart and is much smaller than the first one. The double caniniform dentary teeth are as large as the first tooth and are set in alveoli 3 + 4, which are confluent and raised above the tooth row. Dentary alveoli 5–9 are small, set apart and open on a concave area of the tooth row. Thecodont implantation prevails for the first 14 alveoli. From the fifteenth to the last dentary alveolus the teeth are set in a groove. Occlusal pits could not be detected in the dentary. Lingual to the molariform dentition, the splenial is distinctly enlarged, forming a shelf. A coronoid seems present, as evidenced from the right mandible in medial view, between the surangular and the dentary. For preservational reasons, it is not possible to provide more morphological details. The angular best preserves its general shape on the right mandible and occupies the lower half of its posterior margin. The surangular–angular suture extends nearly horizontally posteriorly to the end of the mandible. The angular and surangular hide the articular and retroarticular process in lateral view. In lateral view, the posteroventral margin of the angular is convex; its posterodorsal margin is devoid of ornamentation. In ventral view, the angular consists of a mediolaterally thin ridge, which corresponds to the

attachment point of the M. pterygoideus posterior. Also in ventral view, the angular sends an anterior process between the dentary and splenial. Medially, the posterior wall of the angular accommodates the descending process of the articular. On the left mandible, the surangular has a horizontal dorsal margin. This margin is simple with no obvious muscle scars and is mediolaterally thin. The combined height of the surangular and angular is about twice that of the dentary ramus. The contact between the surangular and dentary is poorly preserved and it is not possible to assess its sutural pattern. Nevertheless, the surangular does not reach the level of the posterior dentary tooth row. In lateral view, the posterior part of the surangular slopes ventrally to form a posterior process that follows and covers the medially placed retroarticular process. The articular sutures to the medial side of the surangular. In lateral view, only the posterior buttress of the glenoid fossa is visible. The glenoid fossa faces anterodorsally and is formed of two weakly defined sulci of equal dimensions, which are separated by a low anterior pointed process. In front of the lateral sulcus, the anterior surface of the descending articular process is concave and contacts the surangular and eventually the angular at its ventral tip. The retroarticular process projects posteriorly in a lower position than the glenoid fossa. In dorsal or ventral view, the retroarticular process consists of a thin lamina that also projects medially and serves as an obvious attachment area for the M. depressor mandibulae.

Dentition

The dentition of *Bernissartia fagesii* is heterodont and of the tribodont type with blunt and rounded posterior crushing teeth (Buffetaut & Ford 1979; Ősi 2013). All of the teeth possess a mesiodistal carina and finely wrinkled enamel characterized by vertical ridges. From the front to the back of the upper or lower tooth rows, a progressive change in tooth morphology occurs (Fig. 10). The crown progressively diminishes in height and increases in mesiodistal length. The crowns of the premaxillary teeth, maxillary teeth 1–6 and dentary teeth 1–6 are conical, but the crowns of maxillary teeth 7–13 and dentary teeth 7–16 are lanceolate (i.e. with a tooth crown that is triangular in labial or lingual view). The posterior-most teeth (maxillary teeth 14 and 15, dentary teeth 17–19) are bulbous. Those bulbous crowns are mesiodistally longer than high and labiolingually thick. Finally, the last tooth of each tooth row possesses a small rounded crown that is as long as it is high. This tooth is approximately three times smaller than the penultimate tooth. The right upper row, totalling five premaxillary and 16 maxillary teeth, and the left lower row, totalling 20 dentary teeth, are complete. As in extant taxa, the roots are curved lingually with their lingual surface being slightly depressed, whereas their labial surface is convex. The crowns are close to each other, especially in the posterior part of the tooth row, but do not seem to be in contact. The roots of maxillary

Figure 10. The dentition of *Bernissartia fagesii* (IRSNB R46) as revealed through transparent CT reconstructions of the cranium and mandible in **A,** left lateral, **B,** ventral and **C,** right lateral views. Enlargement and details of the extracted right maxillary tooth row in **D,** medial and **E,** lateral views as well as the extracted right dentary tooth row in **F,** medial and **G,** lateral views.

teeth 13–16 do contact each other, however. Although it is less marked in the anterior conical teeth, all of the teeth possess a constriction between the root and the crown. Replacement teeth can be observed as bud crowns in almost every tooth position. These buds develop within the roots of functional teeth. The lingual surface of the functional root shows the typical 'U'-shaped resorption pattern (Poole 1961).

Phylogenetic results

We recovered 10 most parsimonious trees (MPTs) with lengths of 1045 steps (consistency index = 0.332; retention index = 0.663; Fig. 11). Several neosuchian lineages successively fall stem-ward to Eusuchia, with a monophyletic group that includes Goniopholididae, Pholidosauridae + Dyrosauridae, then Paralligatoridae, then *Wannchampsus*, and finally a paraphyletic atoposaurid group (Fig. 11).

Bernissartia fagesii is the sister taxon of *Koumpiodontosuchus aprosdokiti*, supporting a bernissartiid clade (Sweetman *et al.* 2014) that is nested within Eusuchia. Bernissartiidae is the sister group of Susisuchidae (i.e. *Susisuchus anatoceps* and *Isisfordia duncani*) and both of these clades form a polytomy with Hylaeochampsidae. Although Hylaeochampsidae is not monophyletic here, Allodaposuchidae (*Allodaposuchus*, *Agaresuchus*, *Lohuecosuchus*) forms a separate lineage from *Acynodon*, *Iharkutosuchus* and *Hylaeochampsa*. All of the above-mentioned taxa, including Bernissartiidae, are closely related, forming the sister taxon to the crown group, all of which are included within Eusuchia. Inactivating character 178, concerning the lateral contour of the snout, yields similar but slightly different results: the Bernissartiidae form a clade with Susisuchidae, with this clade being the sister group to the crown group.

Discussion

Palate of Bernissartia

The description of *Bernissartia fagesii* Dollo, 1883, from the Early Cretaceous of Belgium, followed the description of another hallmark taxon, *Hylaeochampsa vectiana* Owen, 1874, from the Wealden of England. Until recently, both European taxa were deemed important for comprehending the origin of modern eusuchians (see Pol *et al.* 2009), with *B. fagesii* considered as a derived neosuchian and *H. vectiana* as the basal-most eusuchian (Buffetaut 1975; Clark 1986; Clark & Norell 1992). For this reason, the position of the choanal opening within the palate and vertebral morphology have been central in previous discussions on the affinities of *Bernissartia fagesii* and derived neosuchians (e.g.

Buffetaut 1975; Norell & Clark 1990; Pol *et al.* 2009; Sweetman *et al.* 2014). Here, we will discuss the morphology of the internal choanae based on the new observations allowed by CT data.

Unlike the condition in derived eusuchians, the internal choanal opening of *B. fagesii* is not pterygoid-bound because the palatine contributes to the anterolateral margins of the choana, as a thin lamina connecting ventrally to the pterygoid. The pterygoid hosts most of the choanal recess, extending for most of the median margin of the pterygoidean plate (Fig. 6A). There is no evidence of a recess, but the area is poorly preserved. This pterygoid–palatine-bound choanal configuration is similar to that recently reinterpreted for *Isisfordia duncani* (Turner & Pritchard 2015), as well as a common feature of many neosuchians including *Theriosuchus pusillus* and *Paralligator gradilifrons* (Clark 1986; Turner 2015). Nevertheless, the anterior reach of the choana in *Bernissartia fagesii* is short, unlike in goniopholidids, pholidosaurids, *T. pusillus* or *Rugosuchus nonganensis* where it expands within the suborbital fenestrae. The condition in *B. fagesii* is similar to that of *P. gradilifrons* (Turner 2015) where the choana ends roughly at the level of the suborbital fenestra. Whether it is also similar to *I. duncani* as recently reinterpreted (Turner & Pritchard 2015) should be tested using CT scans of the latter taxon.

Our phylogenetic results support a variable position of the choanal opening in the palate among basal eusuchians, as exemplified here by Bernissartiidae and Susisuchidae, which both contain taxa with pterygoid-bound choanae (Sweetman *et al.* 2014; Leite & Fortier 2018) or with choanae extending into the palatines (Turner & Pritchard 2015; this study). Nevertheless, the condition recently described for *Susisuchus* by Leite & Fortier (2018) requires independent validation in view of the flattened preservation of the specimen. In such a case where the internal choanae open in an anterior position within the palate, cracks could be easily mistaken for the palatine–pterygoid suture, making observations difficult to interpret. A similar issue has been discussed recently in the case of *Isisfordia duncani* (compare the descriptions in Salisbury et al. [2006] with those in Turner & Pritchard [2015]). Basal eusuchians such as hylaeochampsids and members of the crown group offer a palatal configuration less prone to confusion: they possess pterygoid-bound choanae, but these open in a middle or posterior position within the pterygoids (Clark & Norell 1992; Brochu 1999; Martin 2007; Delfino *et al.* 2008a, b; Ősi, 2008; Martin *et al.* 2016a).

In the present phylogeny, the pterygoid-bound configuration of the internal choanae in *Susisuchus* and *Koumpiodontosuchus* may contribute to the unification

of bernissartiids and susisuchids with the rest of Eusuchia. This recovered topology contrasts with a recent study using the same data matrix, which placed susisuchids stem-ward to goniopholidids (Turner 2015; Turner & Pritchard 2015). Indeed, uncertainties remain with respect to the proper extents of the internal choanae in *Isisfordia*, *Susisuchus* and *Koumpiodontosuchus* and new interpretations, for example based on CT data, may help refine our proposed phylogenetic hypothesis. In addition, it is also now recognized that the position of the choanae and the morphology of the vertebrae have evolved multiple times in different neosuchian lineages (Turner & Buckley 2008; Pol *et al.* 2009; Sweetman *et al.* 2014; Leite & Fortier 2018). Although pterygoid-bound choanae do not necessarily characterize eusuchians, according to our results, the participation of the palatine in the choanae does not necessarily disqualify an assignment to basal eusuchians either. Pterygoid-bound choanae were reported in *Mahajangasuchus insignis*, a neosuchian close to Peirosauridae from the Maastrichtian of Madagascar (Turner & Buckley 2008), and as discussed by these authors, there is a strong functional link between platyrostry, tensile stress on the palate and its configuration, as well as feeding style.

Bernissartia and its position among derived neosuchians

The phylogenetic results presented herein should be regarded with caution until anatomical clarifications can be achieved for a number of derived neosuchians and basal eusuchians. Other relevant Cretaceous forms, here mentioned from older to younger deposits, are known only from fragmentary remains and include: *Unasuchus reginae* from the Barremian of Spain (Brinkmann 1992), which is known from cranial and mandibular elements; *Turcosuchus okani* from the ?Barremian of Turkey (Jouve *et al.* 2019), known from a partial mandible and postcranial elements; '*Crocodilus*' *cantabrigiensis* from the Albian 'Greensands' of Great Britain (Seeley 1874), reported from procoelous vertebrae; *Aegyptosuchus peyeri* from the Cenomanian of Egypt (Stromer 1933), known from a skull table and discussed as a possible ally to the enigmatic *Stomatosuchus inermis* from the same formation (Pol *et al.* 2009; see also Sereno & Larsson 2011 and Holliday & Gardner 2012 about stomatosuchid affinities); *Gilchristosuchus palatinus* from the Santonian or Campanian of Alberta (Wu & Brinkman 1993), known from a skull table; and *Dolichochampsa minima* from the Maastrichtian of Argentina (Gasparini & Buffetaut 1980), known from several skull fragments including a braincase and mandibles. Recent reappraisal of the type specimen of *Brillanceausuchus babouriensis* from the

Barremian–Aptian of Cameroon (Michard *et al.* 1990) led Tennant *et al.* (2016) to interpret it as a paralligatorid, a view not supported by the results of Kuzmin *et al.* (2018). Two articulated individuals of *Pietraroiasuchus ormezanoi* from the Albian of Italy were described by Buscalioni et al. (2011), who proposed a close relationship with *Pachycheilosuchus trinquei* from the Barremian of Texas, a taxon known from limited cranial remains (Rogers 2003). Future work on the undescribed neosuchian from the Barremian of Las Hoyas, Spain (see codings in Buscalioni *et al.* 2011) should also prove useful. Indeed, *Hylaeochampsa vectiana* was described from an incomplete skull (Clark & Norell 1992) and several features remain unknown, such as its dentition and mandible. Another potentially important taxon, *Portugalosuchus azenhae*, was recently described from the Cenomanian of west-central Portugal (Mateus *et al.* 2018) and preserves the periorbital area, skull table and palate. The internal choanae are pterygoid-bound and placed in a posterior position, similar to eusuchians such as hylaeochampsids or members of the crown group. Therefore, the above-mentioned taxa represent a potential source for exploring and re-evaluating the evolutionary history of derived neosuchians. For the time being, the position of *B*. *fagesii* within Neosuchia is discussed in the context of recent finds.

Previous studies have found *B*. *fagesii* to be nested among, or at least closely positioned relative to, various neosuchian lineages such as goniopholidids, paralligatorids, atoposaurids, susisuchids and hylaeochampsids (e.g. Norell & Clark 1990; Salisbury *et al.* 2006; Turner 2015; Turner & Pritchard 2015; Kuzmin *et al.* 2018), illustrating our lack of consensus over the position of *B*. *fagesii* and also between these different neosuchian lineages. Here, we recover *B*. *fagesii* as a member of Eusuchia close to *Koumpiodontosuchus* and susisuchids.

B. *fagesii* retains plesiomorphic traits, such as the involvement of the palatine–pterygoid complex in the internal choanae (see above) and the open cranioquadrate passage. The latter's presence has been described in both non-eusuchians and basal eusuchians also. For example, an open cranioquadrate passage is observed in various goniopholidids (e.g. Salisbury *et al.* 1999; Martin *et al.* 2016b), hylaeochampsids (Clark & Norell 1992; Martin 2007; Delfino *et al.* 2008b; Martin *et al.* 2016a), paralligatorids (Turner 2015) and perhaps in atoposaurids (where it is poorly preserved: Martin *et al.* 2014b; Schwarz-Wings *et al.* 2017). This contrasts with the condition in the susisuchid *Isisfordia duncani*, where the cranioquadrate passage is fully enclosed in the quadrate (Salisbury *et al.* 2006). The condition in *B*. *fagesii* also differs from the condition in dyrosaurids (e.g. Brochu *et al.* 2002) and from derived eusuchians, where

the cranioquadrate passage is fully enclosed by the exoccipital and the quadrate.

We do not recover *B. fagesii* as a member of Paralligatoridae. Turner (2015) underlined several characters uniting *Theriosuchus* and Paralligatoridae, including: a slightly sculpted surface of the squamosal lobe showing a prominent depressed area just anterior to the lobe (see also Pol *et al.* 2009); the presence of an orbitonasal sulcus; a midline ridge on the dorsal surface of the frontal and parietal; and a sharp ridge along the lateral surface of the angular. None of these characters are present in *B. fagesii*. Paralligatoridae is further diagnosed by three synapomorphies (Kuzmin *et al.* 2018): of these *B. fagesii* shares the absence of participation of the supraoccipital in the dorsal surface of the skull table, but lacks longitudinal keels restricted to the posterior edge of the dorsal osteoderms and a posteriorly flaring interfenestral bar between the suborbital fenestrae. So, whatever the relationships of Paralligatoridae with Atoposauridae (e.g. Turner 2015; Tennant *et al.* 2016; Kuzmin *et al.* 2018), *B. fagesii* cannot be assigned to either lineage.

B. fagesii is not a close ally of Goniopholididae. Although Goniopholididae share with *B. fagesii* the enlarged double caniniform alveoli for dentary alveoli 3 + 4, this is a symplesiomorphy also observed in derived eusuchians such as *Leidyosuchus*, *Borealosuchus* and *Diplocynodon* (e.g. Brochu 1999; Delfino & Smith 2012; Martin *et al.* 2014a). Goniopholididae differ from *B. fagesii* in, among other characters: having the nasals excluded from the external nares (Salisbury *et al.* 1999; Andrade & Hornung 2011); in possessing a complex pattern of periorbital ridges (Andrade & Hornung 2011); having a straight dentary tooth row (Martin *et al.* 2016b, c); anterolateral processes of the postorbital that project close to the orbital margin of the jugal (e.g. Salisbury & Naish 2011); and in displaying strong anterolateral processes on wider than long dorsal osteoderms (e.g. Martin *et al.* 2016b, c).

Our phylogenetic results and anatomical observations do not support a close affinity between *Bernissartia fagesii* and non-eusuchian neosuchian lineages. Here, we recover a basal neosuchian position for Paralligatoridae close to a polyphyletic Atoposauridae as in another recent work (Tennant *et al.* 2016). As explained above, on the basis of anatomical differences, there is no evidence to relate *B. fagesii* to other neosuchian lineages such as Goniopholididae, Paralligatoridae or Atoposauridae.

Regarding the affinities of *Bernissartia fagesii* with proper eusuchians, our results may appear surprising in view of the close relationships recovered with susisuchids and hylaeochampsids. The rostrum of crocodylomorphs is highly plastic, with several known cases of cranial convergence in distantly related lineages (Brochu 2001). As recovered under one hypothesis here, the close relationship between *B. fagesii* and susisuchids is probably a bias related to snout profile or the possession of a rectilinear tooth row, a condition shared between Susisuchidae and more derived members of Hylaeochampsidae such as *Acynodon* and *Iharkutosuchus* (e.g. Martin 2007; Ősi 2008; Jouve *et al.* 2019). Both taxa also share nasals that participate in the posterior margin of the external nares, the relatively elongate rostrum and the general sutural relationships of the periorbital and skull table areas. Nevertheless, notable differences between susisuchids and hylaeochampsids include tooth row outline, alveolar count, heterodonty and configuration of the cranioquadrate passage. In contrast to susisuchids, the mandible of *B. fagesii* is not rectilinear but shows the double-wave lateral profile matching the premaxillary–maxillary tooth row, a feature commonly observed among derived eusuchians. Moreover, in contrast to susisuchids, *B. fagesii* is markedly heterodont, displaying a caniniform dentition, including confluent anterior dentary alveoli, as well as tribodont posterior teeth. *B. fagesii* has fewer alveolar positions in the maxilla (18) than *Susisuchus* or *Isisfordia duncani* (~20: Salisbury *et al.* 2006; Leite & Fortier 2018). Finally, *B. fagesii* retains a plesiomorphic character with the open cranioquadrate groove, which is closed in *Isisfordia duncani* (Salisbury *et al.* 2006) but unknown in *Susisuchus anatoceps* (Salisbury *et al.* 2003). For the above reasons, it does not seem reasonable to view *B. fagesii* as a susisuchid or as a form close to it. Similarly, removing susisuchids from the analysis results in bernissartiids falling on the stem of the crown group due to the possession of a double wave in the tooth row, a feature widely encountered among members of the crown group, except longirostrine forms. Other traits of *B. fagesii*, such as the possession of enlarged posterior teeth, a medially expanded shelf of the splenial, a quadratojugal forming the posterior corner of the infratemporal fenestra, a jugal bar inset from the lateral surface of the cranium, and a tetraserial arrangement of the dorsal armour, are also shared with *Acynodon* and basal alligatoroids.

Nevertheless, *B. fagesii* is also characterized by a primitive trait: the insertion of the M. pterygoideus posterior along the posteroventral margin of the angular, which is similar to that observed in earlier neosuchians, such as Goniopholididae (Martin *et al.* 2016b), Pholidosauridae (Martin *et al.* 2016c) and Paralligatoridae (e.g. *P. gradilifrons*: see Turner 2015, fig. 5F) where the lateral surface is fully ornamented and the medial surface lacks a developed insertion area. The angular is poorly known in atoposaurids but some specimens might indicate that the situation is similar to other non-eusuchian

neosuchians (see Schwarz-Wings *et al.* 2017). On the other hand, in members of the crown group the insertion area is particularly well developed medially with a large process; moreover, the insertion area also spreads as a smooth surface over the lateral edge of the angular (e.g. Martin *et al.* 2014a, fig. 8).

The possibility of a close relationship between *B. fagesii* and Hylaeochampsidae will have to be tested in future works. The absence of an external mandibular fenestra may represent an apomorphy of Bernissartidae + Hylaeochampsidae, with *Acynodon*, *Allodaposuchus* and *Iharkutosuchus* lacking such a fenestra (Martin *et al.* 2016a). The mandible is unknown in *Hylaeochampsa* but another possible eusuchian, *Unasuchus reginae,* also lacks an external mandibular fenestra (Brinkmann 1992) and was recently recovered as a member of Hylaeochampsidae (Jouve *et al.* 2019). All other eusuchians from the crown group possess an external mandibular fenestra and its reported presence in the susisuchid *I. duncani* (Salisbury *et al.* 2006) is at odds with our results placing Susisuchidae with Hylaeochampsidae and Bernissartidae (presence/absence of the external mandibular fenestra is unknown in *S. anatoceps*; Salisbury *et al.* 2003). However, according to Leite & Fortier (2018), an external mandibular fenestra is absent in *S. anatoceps*.

Despite sharing several features, *B. fagesii* differs from Hylaeochampsidae in a number of characters, beginning with the configuration of the internal choanae in the palate (see above). Other differences include the participation of the nasals in the external nares or the position of the foramen aereum on the quadrate. On the distal margin of the quadrate, the foramen aereum is clearly visible and opens on the mediodorsal margin of the medial hemicondyle as in *Paralligator gradilifrons* and crocodyloids. This foramen is dorsally placed in *Allodaposuchus* (Delfino *et al.* 2008a; Martin *et al.* 2016a) and also among alligatoroids, but not in crocodyloids (Brochu 1999).
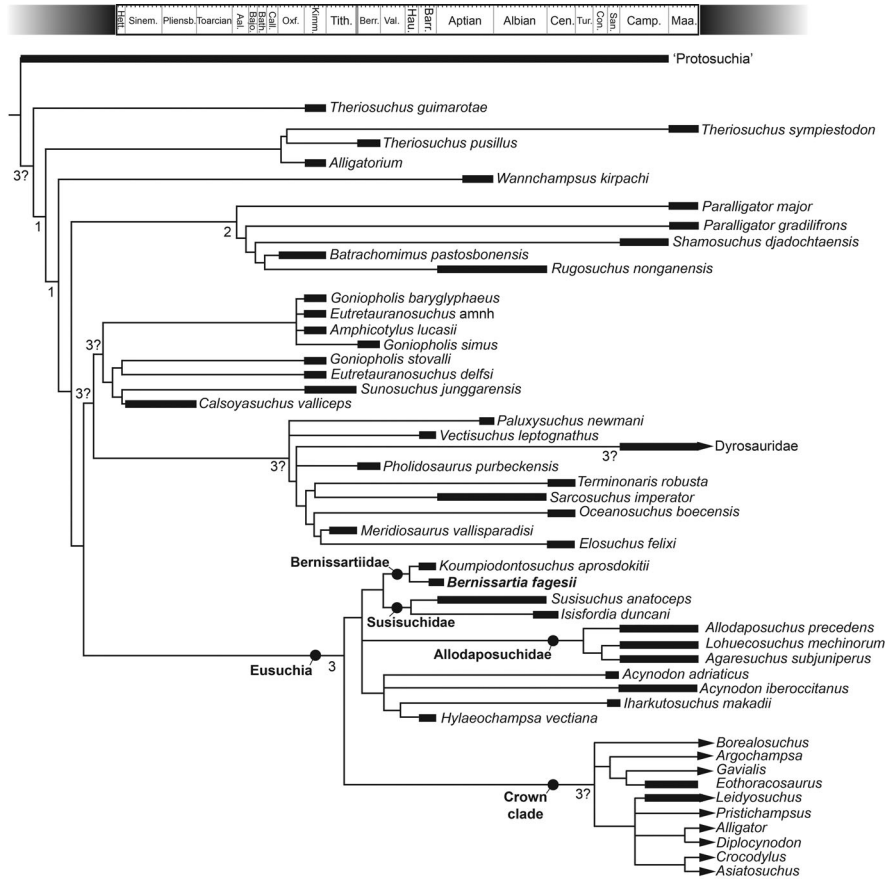
Our phylogenetic analysis recovers *B. fagesii* as a member of Eusuchia, in a clade containing *Susisuchus*, *Isisfordia*, *Koumpiodontosuchus*, *Acynodon*, *Hylaeochampsa*, *Iharkutosuchus* and Allodaposuchidae. In contrast to members of the crown group, hylaeochampsids, bernissartiids and susisuchids evolved with various configurations of the choanae, the cranioquadrate passage and the vertebrae, characters that may no longer be used in the definition of Eusuchia. Our results support the hypothesis of a lineage of endemic basal eusuchians that populated the European archipelago during the Cretaceous. The relationship of susisuchids, from southern landmasses, with hylaeochampsids and bernissartiids, from Europe, requires further investigation, notably by retrieving new specimens from the field, including Cretaceous forms from Gondwana such as *Aegyptosuchus*, *Brillanceausuchus*, *Dolichochampsa* and *Stomatosuchus*.

Spatiotemporal distribution of Bernissartiidae

The distribution of *Bernissartia fagesii* was reviewed by Buffetaut & Ford (1979), who based their identifications largely on isolated teeth and carefully referred these occurrences to bernissartiids. Since then, rare but nearly complete cranial remains are providing a clearer picture. Notably, the recent description of *Koumpiodontosuchus aprosdokitii* from the Barremian of the Isle of Wight, UK (Sweetman *et al.* 2014) highlights that a tribodont dentition is not only present in *Bernissartia fagesii* but in another genus of similar age. As a result, assessments of the distribution of *Bernissartia fagesii* based on isolated teeth should be regarded with caution until the teeth of both taxa are compared. Given the phylogenetic topology recovered here, it seems safe for the time being to refer isolated tribodont teeth from the Jurassic and Cretaceous of Europe to Bernissartiidae indet. Reports of teeth assigned to *Bernissartia* sp. from the Kimmeridgian of Guimarota, Portugal (Brinkmann 1989), the Berriasian of the Purbeck Limestone Group, UK (Salisbury 2002), the Berriasian of Cherves-de-Cognac, France (Mazin & Pouech, 2008), and the Berriasian of Denmark (Schwarz-Wings *et al.* 2009) are all significantly older than the complete skull from the Barremian of the Isle of Wight (Sweetman *et al.* 2014) or from the complete specimen referred herein (see also Buffetaut 1975; Norell & Clark 1990). Cranial remains that would clarify the relationships of these specimens with younger recognized taxa, such as *Bernissartia fagesii* and *Koumpiodontosuchus aprosdokitii*, have yet to be reported from Berriasian deposits. Clarifying the age of the skull referred to *Bernissartia fagesii* from the Berriasian (?)–lower Aptian of Galve, Spain (Buscalioni *et al.* 1984; Buscalioni & Sanz 1990) will be helpful in that regard. That bernissartiids were common in the Barremian faunas of western Europe is now ascertained by their occurrence at different localities in Spain (Brinkmann 1992; Buscalioni *et al.* 2008).

Bernissartiid teeth have been reported outside Europe from the Albian Trinity Formation, Texas (Langston 1974; Thurmond 1974) and the Albian–Cenomanian Cedar Mountain Formation, Utah (Cifelli *et al.* 1999). Isolated tribodont teeth have also been attributed to ?*Bernissartia* from the Middle and Upper Saurian Beds at Tendaguru, Tanzania, which are dated to late Kimmeridgian and post-Tithonian–pre-Valanginian, respectively (Heinrich *et al.* 2001). Although it may be possible that the group occurs elsewhere, this record

Figure 11. Stratigraphically calibrated strict consensus tree of derived neosuchians as recovered in this work including the relationships of Paralligatoridae, Goniopholididae, Pholidosauridae, Hylaeochampsidae and the crown clade. Note that Atoposauridae are not monophyletic. Numbers refer to Bremer support indices.

should be re-evaluated because convergent forms with tribodont teeth are known to exist (see below). For now, current evidence restricts the occurrence of Bernissartiidae to the Kimmeridgian–Aptian interval. The occurrence of *Bernissartia fagesii* itself is restricted to the late Barremian–early Aptian of Belgium, but this range may be expanded with datation of the Galve specimen.

As noted previously by several authors, bernissartiids often co-occur in the same deposits with goniopholidids and pholidosaurids (e.g. Salisbury 2002; Mazin & Pouech 2008; Schwarz-Wings *et al.* 2009) implying spatial and/or niche partitioning to explain such high local crocodylomorph biodiversity (Martin *et al.* 2016c).

Diet of *Bernissartia* and other tribodont forms

The distinctive dental morphology of *Bernissartia fagesii* has usually been considered to indicate a preference for feeding on hard-shelled organisms. Buffetaut & Ford (1979) did not favour a diet of turtles due to the small size of *B. fagesii*. Arguments for or against chelinovory

among blunt-toothed crocodylomorphs have often been discussed with indirect evidence (e.g. Carpenter & Lindsey 1980; Bartels 1984) that does not satisfactorily support any hypothesis. A recent study of traces on a pleurosternid shell provides evidence for chelonivorous habits in the large generalist-morphotype genus *Goniopholis* (Gônet *et al.* 2019). Therefore, blunt posterior teeth are not essential for subduing hard-shelled prey and modern species with a generalist appearance feed on turtles when they are available. With respect to *B. fagesii*, Buffetaut & Ford (1979) considered a specialized mollusc-eating diet, as the Wealden deposits of the Isle of Wight yield various freshwater invertebrates including lamellibranchs, gastropods and planorbids, a hypothesis shared by Sweetman *et al.* (2014) regarding the diet of the other bernissartid *Koumpiodontosuchus aprosdokitii*. Although this might be possible, *B. fagesii* is not as brevirostrine as other small eusuchians, such as *Acynodon* (e.g. Martin 2007; Delfino *et al.* 2008b) and *Gnathusuchus*: the latter is interpreted as a mollusc-crusher as evidenced by punctured molluscs found in the same deposits (Salas-Gismondi *et al.* 2015).

Another indicator of diet is body size, because diet changes through ontogeny as observed in a variety of modern species (Cott 1961; Magnusson *et al.* 1987; see references in Grigg & Kirshner 2015). Accordingly, diet in crocodylians can be directly related to body size increase, ranging from insects, amphibians, crustaceans and/or molluscs to fishes, reptiles, birds and mammals. The frequency histograms based on the proportions of food items retrieved from the stomach contents of *Crocodylus niloticus* are useful (Cott 1961, fig. 34). They reveal that for a body length of <1 m, i.e. corresponding to that of *Bernissartia fagesii*, the diet contained a high proportion of insects and crustaceans. Does that mean that *B. fagesii* was relying exclusively on such organisms? The question remains open until direct evidence becomes available. Nevertheless, it should be remembered that modern crocodylians are opportunistic and will feed on whatever is available to them (see discussion in Grigg & Kirshner 2015) and there is no reason to think otherwise for extinct species. In fact, the anterior conical teeth in *B. fagesii* would have allowed prey capture of any type within the limits of mouth holding. The closest modern analogue to *B. fagesii* is the genus *Osteolaemus*, from the equatorial forests of Africa, which displays a blunt posterior dentition and does not surpass 2 m in total body length. Its diet has been described as opportunistic, with stomach contents containing crustaceans, insects, amphibians and small mammals (Pauwels *et al.* 2007; Shirley *et al.* 2016). Again, in the case of *B. fagesii*, it is difficult to evaluate the diet of an extinct taxon where stomach contents are absent, but *Osteolaemus* might be a good analogue for understanding the diet of *B. fagesii*.

All eusuchians with a tribodont dentition are less than 2 m in total body length, including Cretaceous, Paleogene and Neogene forms (e.g. see review in Ősi 2008). If tribodonty is constrained by resource abundance and body size, ontogenetic growth trajectories may help understand the independent occurrence of the tribodont dentition in distant neosuchian lineages.

Conclusions

Details of the cranial anatomy of *Bernissartia fagesii* are now available on the basis of CT data derived from the best-preserved specimen (IRSNB R46). This will serve as a basis to compare and explore the phylogenetic affinities of Cretaceous representatives of the neosuchian–eusuchian transition. Our exploratory phylogenetic analysis recovers *B. fagesii* as a basal eusuchian, close to Hylaeochampsidae, but in a context where a consensus over the relationships of the different neosuchian lineages has not yet been achieved. Although these results should be critically re-evaluated in the light of new discoveries and additional phylogenetic codings, we point out an important result in recovering no support for a relationship of *B. fagesii* with either Atoposauridae, Paralligatoridae or Goniopholididae. Although not resolvable here, the phylogenetic position of *B. fagesii* might still lie somewhere among derived non-eusuchian neosuchians or close to basal eusuchians. From a palaeoecological point of view, the tribodont dentition of *B. fagesii* is reminiscent of other small forms from different ages and localities, highlighting repeated occurrences during the evolutionary history of derived neosuchians. As indicated by its small size, *B. fagesii* may have regularly fed on small molluscs, insects and crustaceans but also on small vertebrates such as frogs or lizards. Many Cretaceous eusuchians reached relatively small body sizes (*c.* 1 m) at adulthood. The evolutionary significance of tribodonty and small body size will have to be explored in the light of ecological and developmental constraints.

Supplemental material

Supplemental material for this article can be accessed at: http://dx.doi.org/10.1080/14772019.2020.1731722.

ORCID

Jeremy E. Martin ⓘ http://orcid.org/0000-0001-9159-645X
Thierry Smith ⓘ http://orcid.org/0000-0002-1795-2564
Massimo Delfino ⓘ http://orcid.org/0000-0001-7836-7265

References

Andrade, M. B. de & **Hornung, J. J.** 2011. A new look into the periorbital morphology of *Goniopholis* (Mesoeucrocodylia: Neosuchia) and related forms. *Journal of Vertebrate Paleontology*, **31**, 352–368. doi:10.1080/02724634.2011.550353

Bartels, W. S. 1984. Osteology and systematic affinities of the horned alligator *Ceratosuchus* (Reptilia, Crocodilia). *Journal of Paleontology*, **58**, 1347–1353.

Benton, M. J. & **Clark, J. M.** 1988 Archosaur phylogeny and the relationships of the Crocodilia. Pp. 295–338 in M. J. Benton (ed.) *The phylogeny and classification of tetrapods. Volume 1, Systematics association special volume no. 35A Amphibians, reptiles, birds*. Clarendon Press Oxford, UK,

Brinkmann, W. 1989. Vorläufige Mitteilung über die Krokodilier-Faunen aus dem Ober-Jura (Kimmeridgium) der Kohlegrube Guimarota, bei Leiria (Portugal) und der Unter-Kreide (Barremium) von Uña (Provinz Cuenca, Spanien). *Documenta Naturae*, **56**, 1–28.

Brinkmann, W. 1992. Die Krokodilier-Fauna aus der Unter-Kreide (Ober-Barremium) von Uña (Provinz, Cuenca, Spanien). *Berliner Geowissenschaftliche Abhandlungen, Reihe E, Band*, **5**, 1–123.

Brochu, C. A. 1999. Phylogenetics, taxonomy, and the historical biogeography of Alligatoroidea. *Memoir of the Society of Vertebrate Paleontology*, **6**, 9–100. doi:10.2307/3889340

Brochu, C. A. 2001. Crocodylian snouts in space and time: phylogenetic approaches toward adaptive radiation. *American Zoologist*, **41**, 564–585. doi:10.1093/icb/41.3.564

Brochu, C. A., **Bouare, M. L.**, **Sissoko, F.**, **Roberts, E. M.** & **O'Leary, M. A.** 2002. A dyrosaurid crocodyliform braincase from Mali. *Journal of Paleontology*, **76**, 1060–1071. doi:10.1666/0022-3360(2002)076<1060:ADCBFM>2.0.CO;2

Brusatte, S. L., **Muir, A.**, **Young, M. T.**, **Walsh, S.**, **Steel, L.** & **Witmer, L. M.** 2016. The braincase and neurosensory anatomy of an Early Jurassic marine crocodylomorph: implications for crocodylian sinus evolution and sensory transitions. *The Anatomical Record*, **299**, 1511–1530. doi:10.1002/ar.23462

Buffetaut, E. 1975. Sur l'anatomie et la position systématique de *Bernissartia fagesii* Dollo, L., 1883, crocodilien du Wealdien de Bernissart, *Belgique*. Bulletin de l'Institut Royal des Sciences Naturelles de Belgique, **51**, 1–20.

Buffetaut, E. & **Ford, R. L. E.** 1979. The crocodilian *Bernissartia* in the Wealden of the Isle of Wight. *Palaeontology*, **22**, 905–912.

Bultynck, P. 1989. *Bernissart et les Iguanodons*. L'institut Royal des Sciences naturelles de Belgique, Brussels, 115 pp.

Buscalioni, A. D., **Buffetaut, E.** & **Sanz, J. L.** 1984. An immature specimen of the crocodilian *Bernissartia* from the Lower Cretaceous of Galve (*Province of Teruel, Spain)*. Palaeontology, **27**, 809–813.

Buscalioni, A. D. & **Sanz, J. L.** 1990. The small crocodile *Bernissartia fagesii* from the Lower Cretaceous of Galve (Teruel, Spain). *Bulletin de l'Institut Royal des Sciences Naturelles de Belgique*, **60**, 129–150.

Buscalioni, A. D., **Frenegal, M. A.**, **Bravo, A.**, **Poyato-Ariza, F. J.**, **Sanchíz, B.**, **Báez, A. M.**, **Cambra Moo, O.**, **Martín Closas, C.**, **Evans, S. E.** & **Marugán Lobón, J.** 2008. The vertebrate assemblage of Buenache de la Sierra (Upper Barremian of Serrania de Cuenca, Spain) with insights into its taphonomy and palaeoecology. *Cretaceous Research*, **29**, 687–710. doi:10.1016/j.cretres.2008.02.004

Buscalioni, A. D., **Piras, P.**, **Vullo, R.**, **Signore, M.** & **Barbera, C.** 2011. Early eusuchian Crocodylomorpha from the vertebrate-rich Plattenkalk of Pietraroia (lower Albian, southern Apennines, Italy). *Zoological Journal of the Linnean Society*, **163**, S199–S227. doi:10.1111/j.1096-3642.2011.00718.x

Carpenter, K. & **Lindsey, D.** 1980. The dentary of *Brachychampsa montana* Gilmore (Alligatorinae; Crocodylidae), a Late Cretaceous turtle-eating alligator. *Journal of Paleontology*, **54**, 1213–1217.

Cifelli, R. L., **Nydam, R. L.**, **Weil, A.**, **Eaton, J. G.**, **Kirkland, J. I.** & **Madsen, S. K.** 1999. Medial Cretaceous vertebrates from the Cedar Mountain Formation, Emery County, Utah: the Mussentuchit local fauna. *Miscellaneous Publication, Utah Geological Survey*, **99**(1), 219–242.

Clark, J. M. 1986. *Phylogenetic relationships of the crocodylomorph archosaurs*. Unpublished PhD dissertation. University of Chicago, 556 pp.

Clark, J. M. & **Norell, M. A.** 1992. The Early Cretaceous crocodylomorph *Hylaeochampsa vectiana* from the Wealden of the Isle of Wight. *American Museum Novitates*, **3032**, 1–19. http://digitallibrary.amnh.org/handle/2246/5002

Cott, H. B. 1961. Scientific results of an enquiry into the ecology and economic status of the Nile Crocodile (*Crocodylus niloticus*) in Uganda and Northern Rhodesia. *Transactions of the Zoological Society of London*, **29**, 211–356.

Delfino, M., **Codrea, V.**, **Folie, A.**, **Dica, P.**, **Godefroit, P.** & **Smith, T.** 2008a. A complete skull of *Allodaposuchus precedens* Nopcsa, 1928 (Eusuchia) and a reassessment of the morphology of the taxon based on the Romanian remains. *Journal of Vertebrate Paleontology*, **28**, 111–122.

Delfino, M., **Martin, J. E.** & **Buffetaut, E.** 2008b. A new species of *Acynodon* (Crocodylia) from the Upper Cretaceous (Santonian-Campanian) of Villaggio del Pescatore, *Italy*. Palaeontology, **51**, 1091–1106. doi:10.1111/j.1475-4983.2008.00800.x

Delfino, M. & **Smith, T.** 2012. Reappraisal of the morphology and phylogenetic relationships of the middle Eocene alligatoroid *Diplocynodon deponiae* (Frey, Laemmert, and Riess, 1987) based on a three-dimensional specimen. *Journal of Vertebrate Paleontology*, **32**, 1358–1369. doi:10.1080/02724634.2012.699484

Dollo, L. 1883. Première note sur les crocodiliens de Bernissart. *Bulletin de l'Institut Royal des Sciences Naturelles de Belgique*, **2**, 309–340.

Gasparini, Z. & **Buffetaut, E.** 1980. *Dolichochampsa minima*, n. g., n. sp., a representative of a new family of eusuchian crocodiles from the Late Cretaceous of northern Argentina. *Neues Jahrbuch für Geologie und Paläontologie, Monatshefte*, **1980**, 257–271.

Godefroit, P., **Yans, J.** & **Bultynck, P.** 2012. Bernissart and the Iguanodons: historical perspective and new investigations. Pp. 3–20 in P. Godefroit (ed.) *Bernissart*

dinosaurs and Early Cretaceous terrestrial ecosystems. Indiana University Press, Bloomington and Indianapolis.

Goloboff, P. A., **Farris, J. S.** & **Nixon, K. C.** 2008. TNT, a free program for phylogenetic analysis. *Cladistics*, **24**, 774–786. doi:10.1111/j.1096-0031.2008.00217.x

Gônet, J., **Rozada, L.**, **Bourgeais, R.** & **Allain, R.** 2019. Taphonomic study of a pleurosternid turtle shell from the Early Cretaceous of Angeac-Charente, southwest France. *Lethaia.*, **52**, 232–243. doi:10.1111/let.12309

Grigg, G. & **Kirshner, D.** 2015. *Biology and evolution of crocodylians*. CSIRO Publishing, Clayton South, Australia 672 pp.

Heinrich, W.-D., **Bussert, R.**, **Aberhan, M.**, **Hampe, O.**, **Kapilima, S.**, **Schrank, E.**, **Schultka, S.**, **Maier, G.**, **Msaky, E.**, **Sames, B.** & **Chami, R.** 2001. The German-Tanzanian Tendaguru expedition 2000. *Fossil Record*, **4**, 223–237.

Holliday, C. M. & **Gardner, N. M.** 2012. A new eusuchian crocodyliform with novel cranial integument and its significance for the origin and evolution of Crocodylia. *PLoS ONE*, **7**, e30471. doi:10.1371/journal.pone.0030471

Iordansky, N. N. 1973. The skull of the Crocodylia. Pp. 201–262 in C. Gans & T. S. Parsons (eds) *Biology of the Reptilia, Volume 1. Morphology A*. Academic Press, London and New York.

Jouve, S., **Sarigül, V.**, **Steyer, J.-S.** & **Sen, S.** 2019. The first crocodylomorph from the Mesozoic of Turkey (Barremian of Zonguldak) and the dispersal of the eusuchians during the Cretaceous. *Journal of Systematic Palaeontology*, **17**, 111–128. doi:10.1080/14772019.2017.1393469

Kuzmin, I. T., **Skutschas, P. P.**, **Boitsova, E. A.** & **Sues, H.-D.** 2018. Revision of the large crocodyliform *Kansajsuchus* (Neosuchia) from the Late Cretaceous of Central Asia. *Zoological Journal of the Linnean Society*, **185**, 335–387. doi:10.1093/zoolinnean/zly027

Langston, W. 1974. Non-mammalian Comanchean tetrapods. *Geoscience and Man*, **8**, 77–102.

Leite, K. J. & **Fortier, D. C.** 2018. The palate and choanae structure of the *Susisuchus anatoceps* (Crocodyliformes, Eusuchia): phylogenetic implications. *PeerJ*, **6**, e5372. doi:10.7717/peerj.5372

Magnusson, W. E., **da Silva, E. V.** & **Lima, A. P.** 1987. Diets of Amazonian crocodilians. *Journal of Herpetology*, **21**, 85–95. doi:10.2307/1564468

Martin, J. E. 2007. New material of the Late Cretaceous globidontan *Acynodon iberoccitanus* (Crocodylia) from southern France. *Journal of Vertebrate Paleontology*, **27**, 362–372.

Martin, J. E. & **Buffetaut, E.** 2012. The maxillary depression of Pholidosauridae: an anatomical study. *Journal of Vertebrate Paleontology*, **32**, 1442–1446. doi:10.1080/02724634.2012.697504

Martin, J. E., **Smith, T.**, **de Lapparent de Broin, F.**, **Escuillié, F.** & **Delfino, M.** 2014a. Late Palaeocene eusuchian remains from Mont de Berru, France, and the origin of the alligatoroid *Diplocynodon*. *Zoological Journal of the Linnean Society*, **172**, 867–891. doi:10.1111/zoj.12195

Martin, J. E., **Rabi, M.**, **Csiki-Sava, Z.** & **Vasile, S.** 2014b. Cranial morphology of *Theriosuchus sympiestodon* (Mesoeucrocodylia, Atoposauridae) and the widespread occurrence of *Theriosuchus* in the Late Cretaceous of Europe. *Journal of Paleontology*, **88**, 444–456. doi:10.1666/13-106

Martin, J. E., **Delfino, M. Garcia, G.**, **Godefroit, P.**, **Berton, S.** & **Valentin, X.** 2016a. New specimens of *Allodaposuchus precedens* from France: intraspecific variability and the diversity of European Late Cretaceous eusuchians. *Zoological Journal of the Linnean Society*, **176**, 607–631. doi:10.1111/zoj.12331

Martin, J. E., **Delfino, M.** & **Smith, T.** 2016b. Osteology and affinities of Dollo's goniopholidid (Mesoeucrocodylia) from the Early Cretaceous of Bernissart, Belgium. *Journal of Vertebrate Paleontology*, **36**, e1222534. doi:10.1080/02724634.2016.1222534

Martin, J. E., **Raslan-Loubatié, J.** & **Mazin, J. M.** 2016c. Cranial anatomy of *Pholidosaurus purbeckensis* from the Lower Cretaceous of France and its bearing on pholidosaurid affinities. *Cretaceous Research*, **66**, 43–59. doi:10.1016/j.cretres.2016.05.008

Mateus, O., **Puértolas-Pascual, E.** & **Callapez, P. M.** 2018. A new eusuchian crocodylomorph from the Cenomanian (Late Cretaceous) of Portugal reveals novel implications on the origin of Crocodylia. *Zoological Journal of the Linnean Society*, **186**, 501–528. doi:10.1093/zoolinnean/zly064

Mazin, J. M. & **Pouech, J.** 2008. Crocodylomorph microremains from Champblanc (Berriasian, Cherves-de-Cognac, Charente, France). Mid-Mesozoic life and environments. *Documents du Laboratoire de Géologie de Lyon*, **164**, 65–67.

Michard, J. G., **de Broin, F.**, **Brunet, M.** & **Hell, J. F.** 1990. Le plus ancien crocodilien néosuchien spécialisé à caractères 'eusuchiens' du continent africain (Crétacé inférieur, Cameroun). *Comptes Rendus de l'Académie des Sciences, Paris, Series II*, **311**, 365–371.

Norell, M. A. & **Clark, J. M.** 1990. A reanalysis of *Bernissartia fagesii*, with comments on its phylogenetic position and its bearing on the origin and diagnosis of the Eusuchia. *Bulletin de l'Institut Royal des Sciences Naturelles de Belgique*, **60**, 115–128.

Ősi, A. 2008. Cranial osteology of *Iharkutosuchus makadii*, a Late Cretaceous basal eusuchian crocodyliform from Hungary. *Neues Jahrbuch für Geologie und Paläontologie, Abhandlungen*, **248**, 279–299. doi:10.1127/0077-7749/2008/0248-0279

Ősi, A. 2013. The evolution of jaw mechanism and dental function in heterodont crocodyliforms. *Historical Biology*, **26**, 1–137. doi:10.1080/08912963.2013.777533

Owen, R. 1874. Monograph on the fossil Reptilia of the Wealden and Purbeck Formations. Suppl. No. 6 (Hylaeochampsa). *Paleontographical Society Monographs*, **27**, 1–7.

Pauwels, O. S. G., **Barr, B.**, **Sanchez, M. L.** & **Burger, M.** 2007. Diet records for the dwarf crocodile, *Osteolaemus tetraspis* in Rabi oil fields and Loango National Park, southwestern Gabon. *Hamadryad*, **31**, 258–264.

Pierce, S. E., **Williams, M.** & **Benson, R. B. J.** 2017. Virtual reconstruction of the endocranial anatomy of the early Jurassic marine crocodylomorph *Pelagosaurus typus* (Thalattosuchia). *PeerJ*, **5**, e3225. doi:10.7717/peerj.3225

Pol, D., **Turner, A. H.** & **Norell, M. A.** 2009. Morphology of the Late Cretaceous crocodylomorph *Shamosuchus djadochtaensis* and a discussion of neosuchian phylogeny as related to the origin of Eusuchia. *Bulletin of the American Museum of Natural History*, **324**, 1–103. doi:10.1206/0003-0090-324.1.1

Poole, D. F. G. 1961. Notes on tooth replacement in the Nile crocodile *Crocodilus niloticus*. *Proceedings of the Zoological Society of London*, **136**, 131–140. doi:10.1111/j.1469-7998.1961.tb06083.x

Rogers, J. V. 2003. *Pachycheilosuchus trinquei*, a new procoelous crocodyliform from the Lower Cretaceous (Albian) Glen Rose Formation of Texas. *Journal of Vertebrate Paleontology*, **23**, 128–145.

Salas-Gismondi, R., **Flynn, J. J.**, **Baby, P.**, **Tejada-Lara, J.**, **Wesselingh, F. P.** & **Antoine, P. -O.** 2015. A Miocene hyperdiverse crocodylian community reveals peculiar trophic dynamics in proto-Amazonian mega-wetlands. *Proceedings of the Royal Society B*, **282**, 20142490. doi:10.1098/rspb.2014.2490

Salisbury, S. W. 2002. Crocodilians from the Lower Cretaceous (Berriasian) Purbeck Limestone Group of Dorset, southern England. *Special Papers in Palaeontology*, **68**, 121–144.

Salisbury, S. W., **Willis, P. M. A.**, **Peitz, S.** & **Sander, P. M.** 1999. The crocodilian *Goniopholis simus* from the Lower Cretaceous of north-western Germany. *Special Papers in Palaeontology*, **60**, 121–148.

Salisbury, S. W., **Frey, E.**, **Martill, D. M.** & **Buchy, M. C.** 2003. A new crocodilian from the Lower Cretaceous Crato Formation of north-eastern Brazil. *Palaeontographica, Abteilung A*, **270**, 3–47.

Salisbury, S. W., **Molnar, R. E.**, **Frey, E.** & **Willis, P. M.** 2006. The origin of modern crocodyliforms: new evidence from the Cretaceous of Australia. *Proceedings of the Royal Society of London B*, **273**, 2439–2448. doi:10.1098/rspb.2006.3613

Salisbury, S. W. & **Naish, D.** 2011. Crocodilians. Pp. 305–369 in D. J. Batten (ed.) *English Wealden fossils*. The Palaeontological Association, London.

Schwarz-Wings, D., **Rees, E.** & **Lindgren, J.** 2009. Lower Cretaceous mesoeucrocodylians from Scandinavia (Denmark and Sweden). *Cretaceous Research*, **30**, 1345–1355. doi:10.1016/j.cretres.2009.07.011

Schwarz-Wings, D., **Raddatz, M.** & **Wings, O.** 2017. *Knoetschkesuchus langenbergensis* gen. nov. sp. nov., a new atoposaurid crocodyliform from the Upper Jurassic Langenberg Quarry (Lower Saxony, northwestern Germany), and its relationships to *Theriosuchus*. *PLoS ONE*, **12**, e0160617. doi:10.1371/journal.pone.0160617

Seeley, H. G. 1874. On cervical and dorsal vertebrae of *Crocodilus cantabrigiensis* (Seeley) from the Cambridge Upper Greensand. *Quarterly Journal of the Geological Society*, **30**, 693–695. doi:10.1144/GSL.JGS.1874.030.01-04.63

Sereno, P. C. & **Larsson, H. C.** 2009. Cretaceous crocodyliforms from the Sahara. *Zookeys*, **28**, 1–143. doi:10.3897/zookeys.28.325

Shirley, M. H., **Burtner, B.**, **Oslisly, R.**, **Sebag, D.** & **Testa, O.** 2016. Diet and body condition of cave-dwelling dwarf crocodiles (*Osteolaemus tetraspis*, Cope 1861) in Gabon. *African Journal of Ecology*, **55**, 411–422. doi:10.1111/aje.12365

Sipla, J. S. & **Spoor, F.** 2008. The physics and physiology of balance. Pp. 227–232 in J. G. M. Thewissen & S. Nummela (eds) *Sensory evolution on the threshold, adaptations in secondarily aquatic vertebrates*. University of California Press Berkeley, USA.

Sookias, R. B. 2019. Exploring the effects of character construction and choice, outgroups and analytical method on phylogenetic inference from discrete characters in extant crocodilians. *Zoological Journal of the Linnean Society*. doi:10.1093/zoolinnean/zlz015

Stromer, E. 1933. Wirbeltierreste der Baharije-Stufe. 12. Die procoelen Crocodilia. *Akademie der Wissenschaften, Mathematisch-Naturwissenschaftliche Abteilung*, **15**, 1–5.

Sweetman, S. C., **Pedreira-Segade, U.** & **Vidovic, S. U.** 2014. A new bernissartiid crocodyliform from the Lower Cretaceous Wessex Formation (Wealden Group, Barremian) of the Isle of Wight, southern England. *Acta Palaeontologica Polonica*, **60**, 257–268.

Tennant, J. P., **Mannion, P. D.** & **Upchurch, P.** 2016. Evolutionary relationships and systematics of Atoposauridae (Crocodylomorpha: Neosuchia): implications for the rise of Eusuchia. *Zoological Journal of the Linnean Society*, **177**, 854–936. doi:10.1111/zoj.12400

Thurmond, J. T. 1974. Lower vertebrate faunas of the Trinity division in north-central Texas. *Geoscience and Man*, **8**, 103–129.

Turner, A. H. 2015. A review of *Shamosuchus* and *Paralligator* (Crocodyliformes, Neosuchia) from the Cretaceous of Asia. *PLoS ONE*, **10**, e0118116. doi:10.1371/journal.pone.0118116

Turner, A. H. & **Buckley, G. A.** 2008. *Mahajangasuchus insignis* (Crocodyliformes: Mesoeucrocodylia) cranial anatomy and new data on the origin of the eusuchian-style palate. *Journal of Vertebrate Paleontology*, **28**, 382–408.

Turner, A. H. & **Pritchard, A. C.** 2015. The monophyly of Susisuchidae (Crocodyliformes) and its phylogenetic placement in Neosuchia. *PeerJ*, **3**, e759. doi:10.7717/peerj.759

Yans, J., **Dejax, J.**, & **Schnyder, J.** 2012. On the age of the Bernissart iguanodons. Pp. 79–86 in P. Godefroit (ed.) *Bernissart dinosaurs and Early Cretaceous terrestrial ecosystems*. Indiana University Press, Bloomington and Indianapolis.

Walker, A. D. 1970. A revision of the Jurassic reptile *Hallopus victor* (Marsh), with remarks on the classification of crocodiles. *Philosophical Transactions of the Royal Society London B*, **257**, 323–372.

Whetstone, K. N. & **Whybrow, P. J.** 1983. A 'cursorial' crocodilian from the Triassic of Lesotho (Basutoland), southern Africa. *Occasional Papers of the Museum of Natural History of the University of Kansas*, **106**, 1–37.

Wu, X. -C. & **Brinkman, D. B.** 1993. A new crocodylomorph of "mesosuchian" grade from the upper Cretaceous upper Milk River Formation, southern Alberta. *Journal of Vertebrate Paleontology*, **13**, 153–160. doi:10.1080/02724634.1993.10011497

Associate Editor: Paul Barrett